Chapter 2
Theoretical Foundations

In this chapter the theoretical foundations of the Standard Model of electroweak interactions, an overview of flavor physics, the theory of the time evolution of neutral mesons and CP violating phenomena are summarised.

2.1 CP Violation in the Standard Model of Particle Physics

In the Standard Model of particle physics, the theories of electromagnetic and weak interactions are unified by the Glashow-Weinberg-Salam (GWS) model [1, 2]. The GWS model describes electroweak interactions by a gauge theory based on the spontaneously broken symmetry groups

$$\mathrm{SU(2)_L} \times \mathrm{U(1)_Y} \xrightarrow{\mathrm{SSB}} \mathrm{U(1)_{em}}. \tag{2.1}$$

The electroweak symmetry breaking is caused by the Higgs mechanism, which generates the $\mathrm{W}^{\pm}$ and Z^0 gauge boson masses and the masses of the fundamental fermions [3–5].

In the following, the basic principles of the Standard Model of electroweak interactions and the spontaneous symmetry breaking by the Higgs mechanism are briefly described. In addition, it will be demonstrated, how in the Yukawa interactions the Higgs field introduces complex couplings to the quark fields, and how in the charged current interactions of quarks these couplings give rise to CP violation. The discussion neglects details of the leptonic sector and focuses on the electroweak interactions of quarks.

The fundamental fermions are organised into three families of quarks and leptons:

$$\begin{pmatrix} \mathrm{u} & \nu_\mathrm{e} \\ \mathrm{d} & \mathrm{e}^- \end{pmatrix}, \quad \begin{pmatrix} \mathrm{c} & \nu_\mu \\ \mathrm{s} & \mu^- \end{pmatrix} \quad \text{and} \quad \begin{pmatrix} \mathrm{t} & \nu_\tau \\ \mathrm{b} & \tau^- \end{pmatrix} \tag{2.2}$$

M. Röhrken, *Time-Dependent CP Violation Measurements*,
Springer Theses, DOI: 10.1007/978-3-319-00726-7_2,

The families have identical gauge interactions, but differ in their flavor quantum numbers and masses. The quarks and leptons form doublets of left-handed and singlets of right-handed fields, denoted in the following by

$$\begin{pmatrix} u_j & \nu_j \\ d_j & e_j \end{pmatrix} \quad \rightarrow \quad \begin{pmatrix} u_{Lj} \\ d_{Lj} \end{pmatrix}, \quad \begin{pmatrix} \nu_{Lj} \\ l_{Lj} \end{pmatrix} \quad \text{and} \quad u_{Rj}, d_{Rj}, l_{Rj} \qquad \text{for } j \in \{1, 2, 3\}, \tag{2.3}$$

where the quark fields are given in the weak eigenstate basis and the index j specifies the family.

The Lagrangian invariant under gauge transformations involves dynamical terms for the quark fields and kinetic terms for the gauge fields B_μ and W^i_μ,

$$\mathcal{L} = \left(\bar{u}_{Lj}, \bar{d}_{Lj}\right) i \not{D} \begin{pmatrix} u_{Lj} \\ d_{Lj} \end{pmatrix} + \bar{u}_{Rj}\, i \not{D} u_{Rj} + \bar{d}_{Rj}\, i \not{D} d_{Rj} - \frac{1}{4} B_{\mu\nu} B^{\mu\nu} - \frac{1}{4} W^i_{\mu\nu} W^{\mu\nu}_i, \tag{2.4}$$

where the symbol $\not{D}$ is defined as $\not{D} := \gamma^\mu D_\mu$. The covariant derivative D_μ introduces couplings of the gauge fields B_μ and W^i_μ to the quark fields, and can be expressed as

$$D_\mu = \partial_\mu - i\, g' Y B_\mu - i\, g T^a W^a_\mu, \tag{2.5}$$

where g' and g are the electroweak coupling constants, and T^a and Y are the generators of the $SU(2)_L$ and the $U(1)_Y$ symmetry groups that introduce the weak isospin and hypercharge.

In U(1), the field strength tensor $B_{\mu\nu}$ is related to the gauge field by

$$B_{\mu\nu} = \partial_\mu B_\nu - \partial_\nu B_\mu, \tag{2.6}$$

and in SU(2), the field strength tensors $W^i_{\mu\nu}$ are related to the gauge fields by

$$W^i_{\mu\nu} = \partial_\mu W^i_\nu - \partial_\nu W^i_\mu - g\, \varepsilon^{ijk}\, W^j_\mu W^k_\nu \qquad \text{for } i \in \{1, 2, 3\}. \tag{2.7}$$

The coupling constants g' and g are related to the Weinberg angle θ_W and the electric charge e by

$$g \sin\theta_W = g' \cos\theta_W = e, \tag{2.8}$$

which provides the unification of weak and electromagnetic interactions.

In this form the vector bosons corresponding to the gauge fields B_μ and W^i_μ are massless and cause long range weak interactions. Furthermore, the couplings are defined as real preventing CP violation to emerge in the interactions.

The Standard Model contains a single SU(2) doublet of a scalar field, that is referred to as the Higgs field and defined by

$$\phi = \begin{pmatrix} \phi^+ \\ \phi^0 \end{pmatrix}. \tag{2.9}$$

The Lagrangian of the scalar field, given by

$$\mathcal{L}_{\text{Higgs}} = \left(D_\mu \phi\right)^\dagger D_\mu \phi - \mu^2 \phi^\dagger \phi - \lambda \left(\phi^\dagger \phi\right)^2, \tag{2.10}$$

is invariant under local SU(2) × U(1) transformations. The covariant derivative D_μ takes the same form as in Eq. 2.5 and introduces the scalar hypercharge in such a way that ϕ^0 does not couple to the photon.

If the scalar field ϕ acquires a non-vanishing vacuum expectation value, for example expressed by

$$\langle 0|\, \phi \,|0\rangle = \frac{1}{\sqrt{2}} \begin{pmatrix} 0 \\ v \end{pmatrix} \quad \text{with} \quad \phi = \frac{1}{\sqrt{2}} e^{i \frac{\sigma^j}{2} \theta^j(x)} \begin{pmatrix} 0 \\ v + h\,(x) \end{pmatrix} \quad \text{and} \quad v = \sqrt{-\frac{\mu^2}{\lambda}}, \tag{2.11}$$

then the $SU(2)_L \times U(1)_Y$ symmetry groups get spontaneously broken down to the $U(1)_{em}$ subgroup, that remains symmetric with respect to the vacuum.

The non-vanishing vacuum expectation value causes the ground state to be degenerated and allows for massless scalar excitations, that can be identified as Nambu-Goldstone bosons [6–8]. The Nambu-Goldstone bosons can be eliminated by making use of the SU(2) invariance of the Lagrangian and removing the dependence on θ^j in Eq. 2.11 by rotations. In the so-called unitarity gauge, the kinetic term of the Lagrangian in Eq. 2.10 adopts the form

$$\begin{aligned} \left(D_\mu \phi\right)^\dagger D_\mu \phi = {} & \frac{1}{2} \left(\partial_\mu h\right) \left(\partial^\mu h\right) \\ & + \frac{1}{8} \left[\left(g' B_\mu - g W_\mu^3\right)^2 + g^2 \left(W_\mu^1\right)^2 + g^2 \left(W_\mu^2\right)^2 \right] (h + v)^2 . \end{aligned} \tag{2.12}$$

The non-vanishing vacuum expectation value of the scalar field gives rise to quadratic terms of the gauge fields and as a consequence the gauge bosons that correspond to these fields acquire a mass. The elimination of the Nambu-Goldstone bosons can be considered as absorbing the degrees of freedom from the Nambu-Goldstone bosons into the longitudinal components of the gauge bosons.

From the Higgs Lagrangian, the fields of three massive vector bosons can be constructed by combinations of the gauge fields B_μ and W_μ^i:

$$\begin{aligned} W_\mu^+ &= \frac{1}{\sqrt{2}} \left(W_\mu^1 - i\, W_\mu^2\right) \\ W_\mu^- &= \frac{1}{\sqrt{2}} \left(W_\mu^1 + i\, W_\mu^2\right) \\ Z_\mu &= \frac{1}{\sqrt{g^2 + g'^2}} \left(g W_\mu^3 - g' B_\mu\right) \end{aligned} \tag{2.13}$$

The fields W_μ^+, W_μ^- and Z_μ can be identified as the heavy vector bosons W^+, W^- and Z^0 mediating the weak interactions. Their masses are related by

$$M_{W^\pm} = M_{Z^0} \cos\theta_W = \frac{1}{2} g v. \tag{2.14}$$

The combination orthogonal to the Z_μ field,

$$A_\mu = \frac{1}{\sqrt{g^2 + g'^2}} \left(g' W_\mu^3 + g B_\mu \right), \tag{2.15}$$

has no mass term and can be identified as the photon.

The couplings of the fermions to the vector bosons can be expressed as the interactions of neutral and charged currents described by the Lagrangian

$$\mathcal{L}_{\text{int}} = \underbrace{e J_{\text{em}}^\mu A_\mu + \frac{g}{\cos\theta_W} \left(J_Z^\mu - \sin^2\theta_W J_{\text{em}}^\mu \right) Z_\mu}_{\text{neutral current interaction (NC)}} - \underbrace{\frac{1}{\sqrt{2}} g \left(J_+^\mu W_\mu^- + J_-^\mu W_\mu^+ \right)}_{\text{charged current interaction (CC)}}, \tag{2.16}$$

where the electromagnetic current J_{em}^μ is given by

$$J_{\text{em}}^\mu = \frac{2}{3} \bar{u}_{Lj} \gamma^\mu u_{Lj} - \frac{1}{3} \bar{d}_{Lj} \gamma^\mu d_{Lj} - \bar{l}_{Lj} \gamma^\mu l_{Lj}, \tag{2.17}$$

the neutral weak current J_Z^μ is given by

$$J_Z^\mu = \frac{1}{2} \left(\bar{u}_{Lj} \gamma^\mu u_{Lj} - \bar{d}_{Lj} \gamma^\mu d_{Lj} - \bar{l}_{Lj} \gamma^\mu l_{Lj} + \bar{\nu}_{Lj} \gamma^\mu \nu_{Lj} \right), \tag{2.18}$$

and the weak charged currents $J_\pm^\mu$ are given by

$$\begin{aligned} J_+^\mu &= \bar{u}_{Lj} \gamma^\mu d_{Lj} + l_{Lj} \gamma^\mu \nu_{Lj}, \\ J_-^\mu &= \bar{d}_{Lj} \gamma^\mu u_{Lj} + \nu_{Lj} \gamma^\mu l_{Lj}. \end{aligned} \tag{2.19}$$

The quark masses arise from the Yukawa interactions with the Higgs field. The Lagrangian of the Yukawa interaction involves the coupling of right-handed quark field singlets via the scalar field ϕ to left-handed quark field doublets and can be written as

$$\mathcal{L}_{\text{Yukawa}} = -Y_{ij}^u \left(\bar{u}_{Lj}, \bar{d}_{Lj} \right) \begin{pmatrix} \phi^{0*} \\ -\phi^- \end{pmatrix} u_{Rj} - Y_{ij}^d \left(\bar{u}_{Lj}, \bar{d}_{Lj} \right) \begin{pmatrix} \phi^+ \\ \phi^0 \end{pmatrix} d_{Rj}, \tag{2.20}$$

where the Yukawa couplings Y^u and Y^d are complex matrices for up-type and down-type quarks. If the scalar field ϕ acquires a non-vanishing vacuum expectation value, then the Yukawa interactions constitute mass terms for the quarks. In the unitarity

gauge, the mass matrices M^u and M^d for the up-type and down-type quarks are proportional to the Yukawa couplings with the scale given by the vacuum expectation value v:

$$\left(M^u\right)_{ij} = \frac{1}{\sqrt{2}} Y^u_{ij}\, v \qquad \text{and} \qquad \left(M^d\right)_{ij} = \frac{1}{\sqrt{2}} Y^d_{ij}\, v \tag{2.21}$$

The mass eigenstates of the quarks are determined by the diagonalisation of the mass matrices with the four unitary 3×3 matrices U^u_L, U^u_R, U^d_L and U^d_R,

$$\begin{pmatrix} m_u & 0 & 0 \\ 0 & m_c & 0 \\ 0 & 0 & m_t \end{pmatrix} = U^u_L M^u U^{u\dagger}_R \qquad \text{and} \qquad \begin{pmatrix} m_d & 0 & 0 \\ 0 & m_s & 0 \\ 0 & 0 & m_b \end{pmatrix} = U^d_L M^d U^{d\dagger}_R . \tag{2.22}$$

The matrices U^u_L, U^u_R, U^d_L and U^d_R transform the left-handed and right-handed quark fields from the weak eigenstate basis, denoted by u and d, to the mass eigenstate basis, denoted in the following by u^m and d^m:

$$\begin{aligned} u^m_L &= U^u_L u_L & \qquad d^m_L &= U^d_L d_L \\ u^m_R &= U^u_R u_R & \qquad d^m_R &= U^d_R d_R \end{aligned} \tag{2.23}$$

The Lagrangian in Eq. 2.16 describing the interactions of quarks with the gauge fields can be written in terms of the quark mass eigenstates. The expressions for the neutral currents retain their form when applying the above transformations. This invariance of the neutral currents with respect to transformations from the weak to the mass eigenstate basis is the reason that no flavor changing neutral currents occur on tree-level and is the fundament of the Glashow-Iliopoulos-Maiani (GIM) mechanism [9].

The charged currents expressed in the mass eigenstate basis are

$$\begin{aligned} J^+_\mu &= \bar{u}_L \gamma^\mu d_L = \bar{u}^m_L \gamma^\mu U^u_L U^{d\dagger}_L d^m_L = \bar{u}^m_L \gamma^\mu V_{CKM} d^m_L \\ J^-_\mu &= \bar{d}_L \gamma^\mu u_L = \bar{d}^m_L \gamma^\mu U^d_L U^{u\dagger}_L u^m_L = \bar{d}^m_L \gamma^\mu V^\dagger_{CKM} u^m_L , \end{aligned} \tag{2.24}$$

where $V_{CKM} = U^u_L U^{d\dagger}_L$ is the unitary 3×3 Cabibbo-Kobayashi-Maskawa (CKM) quark-mixing matrix. The CKM matrix defines the couplings of the $W^\pm$ bosons to the quarks with definite masses in charged current interactions.

For the charged current interactions of quarks, the Lagrangian and the corresponding CP-conjugated Lagrangian expressed by the mass eigenstates of quarks and using the chirality operator $1 - \gamma^5$ are

$$\mathcal{L}_{\text{int}}^{\text{CC}} = -\frac{1}{\sqrt{2}} g \left[\left(\sum_{ij} (V_{CKM})_{ij} \, \bar{u}_i^m \gamma^\mu \left(1 - \gamma^5\right) d_j^m \right) W_\mu^- + \left(\sum_{ij} (V_{CKM})_{ij}^* \, \bar{d}_j^m \gamma^\mu \left(1 - \gamma^5\right) u_i^m \right) W_\mu^+ \right]$$

$$\text{CP} \Updownarrow \tag{2.25}$$

$$\mathcal{L}_{\text{int}}^{\text{CC,CP}} = -\frac{1}{\sqrt{2}} g \left[\left(\sum_{ij} (V_{CKM})_{ij} \, \bar{d}_j^m \gamma^\mu \left(1 - \gamma^5\right) u_i^m \right) W_\mu^+ + \left(\sum_{ij} (V_{CKM})_{ij}^* \, \bar{u}_i^m \gamma^\mu \left(1 - \gamma^5\right) d_j^m \right) W_\mu^- \right].$$

The above equations show, that the symmetry under CP-transformations is only conserved in the charged current interactions of quarks, if $(V_{CKM})_{ij}^* = (V_{CKM})_{ij}$ is satisfied. In 1973, Kobayashi and Maskawa demonstrated that the quark-mixing matrix contains an irreducible complex phase, if there are at least three families of quarks [10]. The complex phase causes $(V_{CKM})_{ij}^* \neq (V_{CKM})_{ij}$ and is the only source of CP violation in the Standard Model. Because of its importance, the properties and implications of the CKM matrix are explained in more detail in the next section.

2.2 The CKM Matrix and the Unitarity Triangle

In charged current interactions given by the Lagrangian in Eq. 2.25, the physical up- and down-type quarks with definite masses couple to the $W^\pm$ bosons according to the involved CKM matrix elements as illustrated in Fig. 2.1.

The CKM matrix relates the mass eigenstates of the down-type quarks to the corresponding weak eigenstates by

$$\begin{pmatrix} d \\ s \\ b \end{pmatrix}_{\substack{\text{weak} \\ \text{basis}}} = \begin{pmatrix} V_{ud} & V_{us} & V_{ub} \\ V_{cd} & V_{cs} & V_{cb} \\ V_{td} & V_{ts} & V_{tb} \end{pmatrix} \begin{pmatrix} d \\ s \\ b \end{pmatrix}_{\substack{\text{mass} \\ \text{basis}}}. \tag{2.26}$$

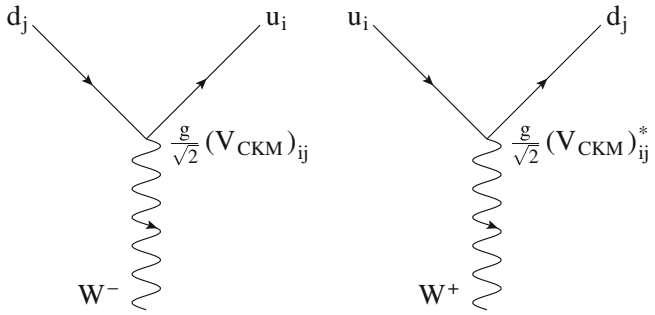

Fig. 2.1 The couplings of the physical up- and down-type quarks to $W^\pm$ bosons in the mass eigenstate basis

In general, a complex $N \times N$ matrix contains $2N^2$ real parameters. The unitarity of the CKM matrix, equivalent to

$$\sum_i (V_{CKM})_{ij} (V_{CKM})^*_{ik} = \delta_{jk} \qquad \text{and} \qquad \sum_j (V_{CKM})_{ij} (V_{CKM})^*_{kj} = \delta_{ik}, \quad (2.27)$$

reduces the number of independent real parameters to N^2.

The phases of the up- and down-type quark fields can be arbitrarily rotated by the transformations

$$u_i \to e^{i\phi^u_i} u_i \qquad \text{and} \qquad d_j \to e^{i\phi^d_j} d_j. \quad (2.28)$$

When applying the above transformations to the CKM matrix elements according to

$$(V_{CKM})_{ij} \to e^{-i\phi^u_i} (V_{CKM})_{ij} e^{i\phi^d_j}, \quad (2.29)$$

then $2N - 1$ relative phases can be eliminated and therefore the matrix contains $(N-1)^2$ independent physical parameters. In general, an orthogonal $N \times N$ matrix can be composed from $\frac{1}{2}N(N-1)$ independent rotation angles. Consequently, the CKM matrix can be constructed from

$$\underbrace{\frac{1}{2}N(N-1)}_{\text{angles}} + \underbrace{\frac{1}{2}(N-1)(N-2)}_{\text{phases}} = \underbrace{(N-1)^2}_{\text{total parameters}} \quad (2.30)$$

parameters [11].

In the case of two fermion families, the CKM matrix contains only one angle and no phase. This case would not allow for CP violation and is equivalent to the two family quark-mixing described by the Cabibbo matrix [12],

$$V_{Cabibbo} = \begin{pmatrix} \cos\theta_C & \sin\theta_C \\ -\sin\theta_C & \cos\theta_C \end{pmatrix}, \quad (2.31)$$

where $\sin\theta_C = |V_{us}| \approx 0.23$ and $\theta_C \approx 13°$ is the Cabibbo angle [13].

In the case of three fermion families as in the Standard Model, the CKM matrix is described by three angles and one complex phase. A representation in analogy to the Cabibbo matrix uses rotations with angles θ_{ij} between family i and j in the parameterisation

$$\mathbf{V}_{CKM} = \begin{pmatrix} 1 & 0 & 0 \\ 0 & c_{23} & s_{23} \\ 0 & -s_{23} & c_{23} \end{pmatrix} \begin{pmatrix} c_{13} & 0 & s_{13}e^{-i\delta} \\ 0 & 1 & 0 \\ -s_{13}e^{i\delta} & 0 & c_{13} \end{pmatrix} \begin{pmatrix} c_{12} & s_{12} & 0 \\ -s_{12} & c_{12} & 0 \\ 0 & 0 & 1 \end{pmatrix} \quad (2.32)$$

$$= \begin{pmatrix} c_{12}c_{13} & s_{12}c_{13} & s_{13}e^{-i\delta} \\ -s_{12}c_{23} - c_{12}s_{23}s_{13}e^{i\delta} & c_{12}c_{23} - s_{12}s_{23}s_{13}e^{i\delta} & s_{23}c_{13} \\ s_{12}s_{23} - c_{12}c_{23}s_{13}e^{i\delta} & -c_{12}s_{23} - s_{12}c_{23}s_{13}e^{i\delta} & c_{23}c_{13} \end{pmatrix}, \quad (2.33)$$

where $c_{ij} = \cos\theta_{ij}$ and $s_{ij} = \sin\theta_{ij}$, and δ is the CP violating phase [14].

The experimental determination of the flavor structure revealed a strong hierarchy in the CKM matrix, which manifests itself in $s_{13} \ll s_{23} \ll s_{12} \ll 1$. The hierarchical structure becomes apparent in a representation in terms of the Wolfenstein parameters λ, A, ρ and η defined by the relations [15]

$$s_{12} = \lambda = \frac{|V_{us}|}{\sqrt{|V_{ud}|^2 + |V_{us}|^2}}, \qquad s_{23} = A\lambda^2 = \lambda \left| \frac{V_{cb}}{V_{us}} \right|, \qquad s_{13}\, e^{i\delta} = A\lambda^3 (\rho + i\,\eta) = V_{ub}^*. \tag{2.34}$$

The expansion of the CKM matrix elements in terms of powers of the parameter $\lambda \approx 0.23$ up to the order of three results in

$$\mathbf{V}_{\mathrm{CKM}} = \begin{pmatrix} 1 - \lambda^2/2 & \lambda & A\lambda^3 (\rho - i\eta) \\ -\lambda & 1 - \lambda^2/2 & A\lambda^2 \\ A\lambda^3 (1 - \rho - i\eta) & -A\lambda^2 & 1 \end{pmatrix} + \mathcal{O}\left(\lambda^4\right). \tag{2.35}$$

This representation reveals the hierarchical structure of the CKM matrix. The diagonal elements represent transitions within the same family and are equal or close to one. The transitions between the first and the second family are suppressed by a factor λ, the transitions between the second and the third family by a factor λ^2, and the transitions between the first and the third family by a factor λ^3. Furthermore, at this order of expansion the complex phase manifests itself in the CKM matrix elements V_{td} and V_{ub}. These elements are important for many physical processes such as the time evolution and the decay of B mesons. This implies CP violation to be possibly sizeable in the charged and neutral B meson system.

The unitarity of the CKM matrix as expressed by Eq. 2.27 results in the following six relations of vanishing CKM matrix element combinations:

$$\underbrace{\mathbf{V}_{ud}^* \mathbf{V}_{us}}_{\mathcal{O}(\lambda)} + \underbrace{\mathbf{V}_{cd}^* \mathbf{V}_{cs}}_{\mathcal{O}(\lambda)} + \underbrace{\mathbf{V}_{td}^* \mathbf{V}_{ts}}_{\mathcal{O}(\lambda^5)} = \delta_{ds} = 0 \tag{2.36}$$

$$\underbrace{\mathbf{V}_{ud} \mathbf{V}_{cd}^*}_{\mathcal{O}(\lambda)} + \underbrace{\mathbf{V}_{us} \mathbf{V}_{cs}^*}_{\mathcal{O}(\lambda)} + \underbrace{\mathbf{V}_{ub} \mathbf{V}_{cb}^*}_{\mathcal{O}(\lambda^5)} = \delta_{uc} = 0 \tag{2.37}$$

$$\underbrace{\mathbf{V}_{us}^* \mathbf{V}_{ub}}_{\mathcal{O}(\lambda^4)} + \underbrace{\mathbf{V}_{cs}^* \mathbf{V}_{cb}}_{\mathcal{O}(\lambda^2)} + \underbrace{\mathbf{V}_{ts}^* \mathbf{V}_{tb}}_{\mathcal{O}(\lambda^2)} = \delta_{sb} = 0 \tag{2.38}$$

$$\underbrace{\mathbf{V}_{td} \mathbf{V}_{cd}^*}_{\mathcal{O}(\lambda^4)} + \underbrace{\mathbf{V}_{ts} \mathbf{V}_{cs}^*}_{\mathcal{O}(\lambda^2)} + \underbrace{\mathbf{V}_{tb} \mathbf{V}_{cb}^*}_{\mathcal{O}(\lambda^2)} = \delta_{ct} = 0 \tag{2.39}$$

$$\underbrace{\mathbf{V}_{td} \mathbf{V}_{ud}^*}_{\mathcal{O}(\lambda^3)} + \underbrace{\mathbf{V}_{ts} \mathbf{V}_{us}^*}_{\mathcal{O}(\lambda^3)} + \underbrace{\mathbf{V}_{tb} \mathbf{V}_{ub}^*}_{\mathcal{O}(\lambda^3)} = \delta_{ut} = 0 \tag{2.40}$$

$$\underbrace{V_{ud}V_{ub}^*}_{\mathcal{O}(\lambda^3)} + \underbrace{V_{cd}V_{cb}^*}_{\mathcal{O}(\lambda^3)} + \underbrace{V_{td}V_{tb}^*}_{\mathcal{O}(\lambda^3)} = \delta_{db} = 0 \tag{2.41}$$

The above relations can be interpreted geometrically as triangles in the complex plane. In the above equations, the order of side lengths in the triangles are specified in terms of the Wolfenstein parameter λ. The first four triangles have sides of very different lengths with ratios of $\lambda{:}\lambda^5 \approx 360$ and $\lambda^2{:}\lambda^4 \approx 19$, and are therefore degenerate. The sides of the two last triangles all have lengths of the order of λ^3, and consequently the triangles have large internal angles of the order of 10°.

The six triangles corresponding to Eqs. 2.36–2.41 all have the same area which is half of the Jarlskog invariant J defined by [16]

$$J = \pm \mathrm{Im}\left[V_{ij}V_{kl}V_{il}^*V_{kj}^*\right] \qquad \text{for } i \neq k,\ l \neq j. \tag{2.42}$$

The Jarlskog invariant is a dimensionless and phase-convention independent measure of the size of CP violation in the Standard Model. The experimentally determined value is $J \approx 3 \times 10^{-5}$ [17]. In combination with the quark masses, it leads to a necessary condition for CP violation given by

$$-2J(m_t^2 - m_c^2)(m_c^2 - m_u^2)(m_u^2 - m_t^2)(m_b^2 - m_s^2)(m_s^2 - m_d^2)(m_d^2 - m_b^2) \neq 0. \tag{2.43}$$

A non-vanishing value of the above relation is necessary for CP violation to emerge in the quark sector [11].

Of particular interest for the physics of B mesons is the triangle given by Eq. 2.41, because each side is related to CKM matrix elements describing b-quark transitions as occurring in CKM-favored and CKM-suppressed B meson decays and in B^0-$\bar{B}^0$ oscillations. The so-called Unitarity Triangle arises by dividing each side by the experimentally best known side, which is $V_{cd}V_{cb}^*$. An illustration of the Unitarity Triangle and the definitions of the angles and sides are shown in Fig. 2.2. The angles α, β and γ of the Unitarity Triangle, also often referred to as ϕ_2, ϕ_1, ϕ_3, are related to CKM matrix elements by

$$\alpha = \phi_2 = \arg\left(-\frac{V_{td}V_{tb}^*}{V_{ud}V_{ub}^*}\right), \tag{2.44}$$

$$\beta = \phi_1 = \arg\left(-\frac{V_{cd}V_{cb}^*}{V_{td}V_{tb}^*}\right), \tag{2.45}$$

$$\gamma = \phi_3 = \arg\left(-\frac{V_{ud}V_{ub}^*}{V_{cd}V_{cb}^*}\right). \tag{2.46}$$

One key objective of flavor physics, in particular of the Belle experiment, is to experimentally overconstrain the Unitarity Triangle by a large variety of independent measurements. The experimental determination of the angles α, β and γ of the Unitarity Triangle is closely related to the measurements of CP violation. The

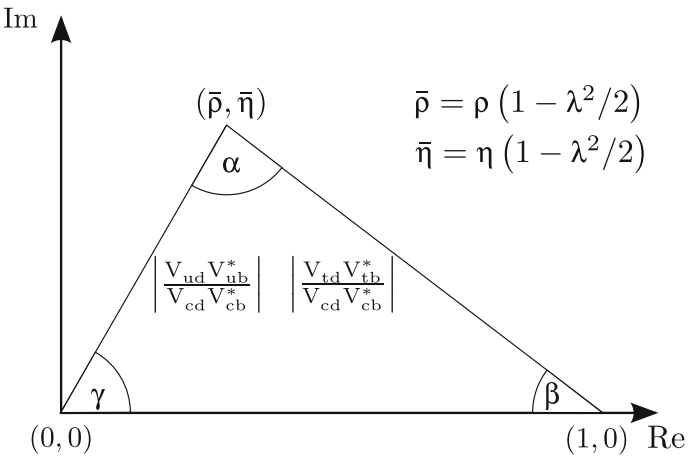

Fig. 2.2 Construction of the Unitarity Triangle in the complex plane

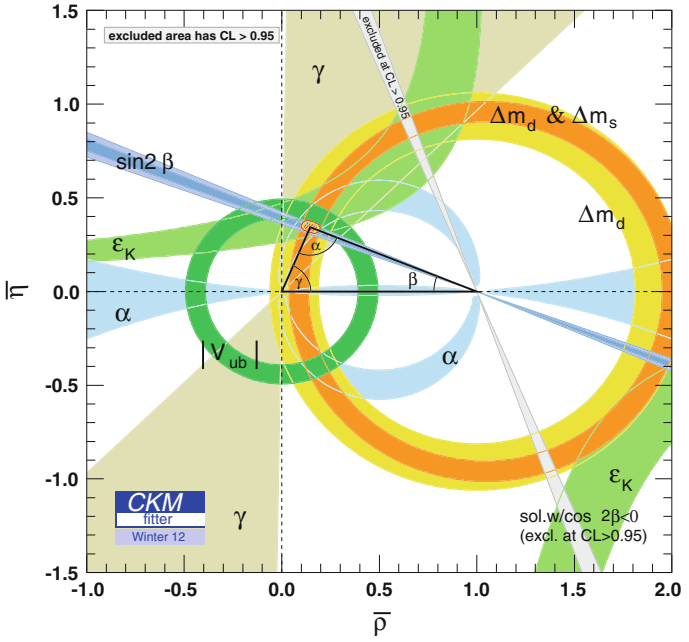

Fig. 2.3 Constraints on the Unitarity Triangle in the $\bar{\rho}\bar{\eta}$-plane at current experimental status. The figure has been provided by the CKMfitter Group [18]

angle β is known at a precision better than 1° from time-dependent measurements of mixing-induced CP violation in $b \to c\bar{c}s$ transitions such as in $B^0 \to J/\Psi K_S^0$ decays, see Sect. 2.6. The objective of the present analysis is the measurement of

time-dependent CP violation in $b \to c\bar{c}d$ transitions, in particular in $B^0 \to D^+D^-$ and $B^0 \to D^{*\pm}D^{\mp}$ decays. The mixing-induced CP violation in $b \to c\bar{c}d$ transitions is closely related to the angle β and can be compared to the reference measurements in $b \to c\bar{c}s$ transitions.

The constraints on the Unitarity Triangle in the $\bar{\rho}\bar{\eta}$-plane at current experimental status are summarised in Fig. 2.3. In total, the flavor part of the Standard Model as determined by constraints from the Unitarity Triangle performs well. Tight constraints come from the mentioned measurements of the angle β, from B^0-$\bar{B}^0$ and B_s^0-$\bar{B}_s^0$ oscillation measurements and from measurements of $|V_{ub}|$ in semileptonic $b \to u$ transitions. In global fits, a few tensions persist which are related to measurements with large uncertainties and need to be confirmed.

The constraints on the Unitarity Triangle and on observables related to the CKM matrix from global fits of available measurements as obtained by the CKMfitter group and the UTfit Collaboration can be found in Refs. [18, 19]. A general summary covering the experimental knowledge about the CKM matrix and the Unitarity Triangle can be found in Ref. [17].

2.3 Time Evolution of Neutral Mesons

The time evolution of weakly decaying neutral mesons is characterised by the effect of particle-antiparticle oscillations. Particle-antiparticle oscillations emerge in different fields of high energy physics and have been experimentally established for neutral mesons and neutrinos. The theoretical explanations for the different kinds of oscillations have all in common, that particles once produced with a definite flavor content, e.g. as a B^0 meson or as a ν_e neutrino, are not the mass eigenstates of their particular dynamic quantum system and evolve over time into mixtures of B^0 and $\bar{B}^0$ mesons or of ν_e, ν_μ and ν_τ neutrinos, respectively.

In the following, the theoretical formalism for the description of the time evolution and mixing of neutral mesons will be introduced with a focus on the B^0 system. The B^0 system is of special importance, because the mixing introduces a phase, that can give rise to large CP violating effects.

In the neutral meson sector, K^0-$\bar{K}^0$, D^0-$\bar{D}^0$, B^0-$\bar{B}^0$ and B_s^0-$\bar{B}_s^0$ oscillations are theoretically described as a 2-level quantum system coupled by higher order weak interactions.

A state that is initially a superposition of P^0 and $\bar{P}^0$ (with $P \in \{K, D, B, B_s\}$), e.g.

$$|\Psi\,(0)\rangle = a(0)|P^0\rangle + b(0)|\bar{P}^0\rangle, \tag{2.47}$$

evolves over time into a different mixture of P^0 and $\bar{P}^0$ and additionally contains contributions of all possible final decay states,

$$|\Psi\,(t)\rangle = a(t)|P^0\rangle + b(t)|\bar{P}^0\rangle + \sum_i c_i(t)|f_i\rangle. \tag{2.48}$$

The time scale of weak interactions that cause particle-antiparticle oscillations is much larger than that of strong or electromagnetic interactions. Following an approximation by Wigner and Weisskopf [20, 21], the time evolution is governed by a Schrödinger equation with an effective Hamiltonian, that does not contain explicitly the couplings to the final-states f_i:

$$i\frac{\partial}{\partial t}\begin{pmatrix} a(t) \\ b(t) \end{pmatrix} = \mathbf{H}\begin{pmatrix} a(t) \\ b(t) \end{pmatrix} \tag{2.49}$$

The effective Hamiltonian $\mathbf{H}$ is not Hermitian due to the possibility of decays of the particles. It is composed of a dispersive and an absorptive part:

$$\mathbf{H} = \mathbf{M} - \frac{i}{2}\mathbf{\Gamma} = \begin{pmatrix} M_{11} & M_{12} \\ M_{21} & M_{22} \end{pmatrix} - \frac{i}{2}\begin{pmatrix} \Gamma_{11} & \Gamma_{12} \\ \Gamma_{21} & \Gamma_{22} \end{pmatrix} \tag{2.50}$$

The diagonal elements of the mass matrix $\mathbf{M}$ and the decay matrix $\mathbf{\Gamma}$ correspond to flavor-conserving $P^0 \leftrightarrow P^0$ and $\bar{P}^0 \leftrightarrow \bar{P}^0$ transitions and the off-diagonal elements to flavor-changing $P^0 \rightarrow \bar{P}^0$ and $\bar{P}^0 \rightarrow P^0$ transitions. The matrices $\mathbf{M}$ and $\mathbf{\Gamma}$ are Hermitian inferring that $M_{12} = M_{21}^*$ and $\Gamma_{12} = \Gamma_{21}^*$. The invariance under CPT-transformations requires $M_{11} = M_{22} =: M$ and $\Gamma_{11} = \Gamma_{22} =: \Gamma$.

The eigenstates of the Hamiltonian are

$$|P_{L,H}\rangle = p\,|P^0\rangle \mp q\,|\bar{P}^0\rangle, \tag{2.51}$$

where the complex coefficients p and q satisfy the normalisation condition $|p|^2 + |q|^2 = 1$ and are given by

$$\begin{aligned} \frac{q}{p} &= \pm\sqrt{\frac{M_{12}^* - \frac{i}{2}\Gamma_{12}^*}{M_{12} - \frac{i}{2}\Gamma_{12}}} \\ &\approx \pm\frac{M_{12}^*}{|M_{12}|}\left(1 - \frac{1}{2}\mathrm{Im}\frac{\Gamma_{12}}{M_{12}}\right). \end{aligned} \tag{2.52}$$

The corresponding eigenvalues are

$$\lambda_{L,H} = M - \frac{i}{2}\Gamma \pm \frac{q}{p}\left(M_{12} - \frac{i}{2}\Gamma_{12}\right). \tag{2.53}$$

$|P_{L,H}\rangle$ represent the physical light (L) and heavy (H) mass eigenstates with well-defined masses $M_{L,H}$ and decay widths $\Gamma_{L,H}$:

$$M_L = \mathrm{Re}\,(\lambda_L) \quad \text{and} \quad \Gamma_L = \mathrm{Im}\,(\lambda_L) \tag{2.54}$$

$$M_H = \mathrm{Re}\,(\lambda_H) \quad \text{and} \quad \Gamma_H = \mathrm{Im}\,(\lambda_H) \tag{2.55}$$

The time evolution of the mass eigenstates can be inferred from the Schrödinger equation:

$$|\,P_{L,H}\,(t)\rangle = e^{-i\mathbf{H}t}|\,P_{L,H}\rangle \tag{2.56}$$

$$= e^{-iM_{L,H}t}e^{-\frac{1}{2}\Gamma_{L,H}t}|\,P_{L,H}\rangle \tag{2.57}$$

The light and heavy eigenstate have a mass difference $\Delta M = M_H - M_L$ and a decay width difference $\Delta\Gamma = \Gamma_L - \Gamma_H$. Neglecting possible CP violation in the mixing by assuming $|\frac{q}{p}| = 1$ the differences are given by $\Delta M = 2|M_{12}|$ and $\Delta\Gamma = 2|\Gamma_{12}|$.

The time evolution for flavor eigenstates can be expressed by the above relations. At time $t = 0$ pure neutral meson states $|P^0\rangle$ and $|\bar{P}^0\rangle$ (with $P \in \{K, D, B, B_s\}$) evolve as

$$|P^0(t)\rangle = g_+(t)|P^0\rangle + \frac{q}{p}g_-(t)|\bar{P}^0\rangle \tag{2.58}$$

$$|\bar{P}^0(t)\rangle = g_+(t)|\bar{P}^0\rangle + \frac{p}{q}g_-(t)|P^0\rangle, \tag{2.59}$$

where

$$g_+(t) = e^{-iMt}e^{-\Gamma t/2}\left[\cosh\left(\frac{\Delta\Gamma t}{4}\right)\cos\left(\frac{\Delta M t}{2}\right) - i\sinh\left(\frac{\Delta\Gamma t}{4}\right)\sin\left(\frac{\Delta M t}{2}\right)\right] \tag{2.60}$$

$$g_-(t) = e^{-iMt}e^{-\Gamma t/2}\left[-\sinh\left(\frac{\Delta\Gamma t}{4}\right)\cos\left(\frac{\Delta M t}{2}\right) + i\cosh\left(\frac{\Delta\Gamma t}{4}\right)\sin\left(\frac{\Delta M t}{2}\right)\right]. \tag{2.61}$$

The functions $g_+(t)$ and $g_-(t)$ have the following properties:

$$\left|g_\pm(t)\right|^2 = \frac{e^{-\Gamma t}}{2}\left[\cosh\left(\frac{\Delta\Gamma t}{2}\right) \pm \cos\left(\Delta M t\right)\right] \tag{2.62}$$

$$g_+^*(t)g_-(t) = \frac{e^{-\Gamma t}}{2}\left[-\sinh\left(\frac{\Delta\Gamma t}{2}\right) + i\sin\left(\Delta M t\right)\right] \tag{2.63}$$

From the above time evolution, the time-dependent decay rates of neutral mesons produced at $t = 0$ in a flavor eigenstate P^0 or $\bar{P}^0$ and decaying to the final-state f can be determined. The time-dependent decay rates are proportional to the absolute square of the involved decay amplitudes:

$$\Gamma\left[P^0(t) \to f\right] \propto \left|\langle f|\mathcal{H}|P^0(t)\rangle\right|^2 \tag{2.64}$$

$$\Gamma\left[\bar{P}^0(t) \to f\right] \propto \left|\langle f|\mathcal{H}|\bar{P}^0(t)\rangle\right|^2 \tag{2.65}$$

The decay rates describing decays to the CP-conjugated state $|\bar{f}\rangle = CP|f\rangle$ are:

$$\Gamma\left[P^0(t) \to \bar{f}\right] \propto \left|\langle \bar{f}|\mathcal{H}|P^0(t)\rangle\right|^2 \tag{2.66}$$

$$\Gamma\left[\bar{P}^0(t) \to \bar{f}\right] \propto \left|\langle \bar{f}|\mathcal{H}|\bar{P}^0(t)\rangle\right|^2 \tag{2.67}$$

For the following discussion, it is advantageous to define the decay amplitudes as

$$A_f := \langle f|\mathcal{H}|P^0\rangle, \quad A_{\bar{f}} := \langle \bar{f}|\mathcal{H}|P^0\rangle, \quad \bar{A}_f := \langle f|\mathcal{H}|\bar{P}^0\rangle \text{ and } \bar{A}_{\bar{f}} := \langle \bar{f}|\mathcal{H}|\bar{P}^0\rangle, \tag{2.68}$$

and to introduce the following ratios defined by

$$\lambda_f := \frac{q}{p}\frac{\bar{A}_f}{A_f} \quad \text{and} \quad \lambda_{\bar{f}} := \frac{q}{p}\frac{\bar{A}_{\bar{f}}}{A_{\bar{f}}}. \tag{2.69}$$

By inserting the time evolution of the flavor eigenstates given by Eqs. 2.58 and 2.59 into Eqs. 2.64–2.67 and making use of the functions $g_+(t)$ and $g_-(t)$ defined in Eqs. 2.60 and 2.61, the time-dependent decay rates are proportional to the following expressions [22]:

$$\Gamma\left[P^0(t) \to f\right] \propto |A_f|^2 e^{-\Gamma t}\left\{\frac{1+|\lambda_f|^2}{2}\cosh\left(\frac{\Delta\Gamma}{2}t\right) + \frac{1-|\lambda_f|^2}{2}\cos(\Delta M t) - \mathrm{Re}(\lambda_f)\sinh\left(\frac{\Delta\Gamma}{2}t\right) - \mathrm{Im}(\lambda_f)\sin(\Delta M t)\right\} \tag{2.70}$$

$$\Gamma\left[\bar{P}^0(t) \to f\right] \propto |A_f|^2 \left|\frac{p}{q}\right|^2 e^{-\Gamma t}\left\{\frac{1+|\lambda_f|^2}{2}\cosh\left(\frac{\Delta\Gamma}{2}t\right) - \frac{1-|\lambda_f|^2}{2}\cos(\Delta M t) - \mathrm{Re}(\lambda_f)\sinh\left(\frac{\Delta\Gamma}{2}t\right) + \mathrm{Im}(\lambda_f)\sin(\Delta M t)\right\} \tag{2.71}$$

$$\Gamma\left[P^0(t) \to \bar{f}\right] \propto \left|\bar{A}_{\bar{f}}\right|^2 \left|\frac{q}{p}\right|^2 e^{-\Gamma t}\left\{\frac{1+\left|\lambda_{\bar{f}}\right|^{-2}}{2}\cosh\left(\frac{\Delta\Gamma}{2}t\right) - \frac{1-\left|\lambda_{\bar{f}}\right|^{-2}}{2}\cos(\Delta M t) - \mathrm{Re}\left(\frac{1}{\lambda_{\bar{f}}}\right)\sinh\left(\frac{\Delta\Gamma}{2}t\right) + \mathrm{Im}\left(\frac{1}{\lambda_{\bar{f}}}\right)\sin(\Delta M t)\right\} \tag{2.72}$$

$$\Gamma\left[\bar{P}^0(t) \to \bar{f}\right] \propto \left|\bar{A}_{\bar{f}}\right|^2 e^{-\Gamma t}\left\{\frac{1+\left|\lambda_{\bar{f}}\right|^{-2}}{2}\cosh\left(\frac{\Delta\Gamma}{2}t\right) + \frac{1-\left|\lambda_{\bar{f}}\right|^{-2}}{2}\cos(\Delta M t) - \mathrm{Re}\left(\frac{1}{\lambda_{\bar{f}}}\right)\sinh\left(\frac{\Delta\Gamma}{2}t\right) - \mathrm{Im}\left(\frac{1}{\lambda_{\bar{f}}}\right)\sin(\Delta M t)\right\} \tag{2.73}$$

The decay rates in Eqs. 2.70–2.73 allow to calculate the time evolution of any neutral weak decay process and are important not only for the mixing, but allow for interference effects that can give rise to CP violation as shown in Sect. 2.4. In the derivation of the decay rates no assumptions except the validity of the CPT theorem

have been applied. Therefore the decay rates are applicable to any weakly decaying neutral meson P^0 or $\bar{P}^0$ (with $P \in \{K, D, B, B_s\}$).

For the oscillations of neutral mesons, the probabilities to observe an initially pure neutral meson P^0 at time $t > 0$ without mixing as a P^0 or with mixing as a $\bar{P}^0$ are given by

$$\begin{aligned} P_{\text{unmixed}}(t) = \left|\langle P^0|P^0(t)\rangle\right|^2 &= \frac{1}{2}e^{-\Gamma t}\left[\cosh\left(\frac{\Delta\Gamma}{2}t\right) + \cos\left(\Delta M t\right)\right] \\ &= \frac{1}{2}e^{-\Gamma t}\left[\cosh\left(y\Gamma t\right) + \cos\left(x\Gamma t\right)\right] \end{aligned} \tag{2.74}$$

$$\begin{aligned} P_{\text{mixed}}(t) = \left|\langle P^0|\bar{P}^0(t)\rangle\right|^2 &= \frac{1}{2}\left|\frac{q}{p}\right|^2 e^{-\Gamma t}\left[\cosh\left(\frac{\Delta\Gamma}{2}t\right) - \cos\left(\Delta M t\right)\right] \\ &= \frac{1}{2}\left|\frac{q}{p}\right|^2 e^{-\Gamma t}\left[\cosh\left(y\Gamma t\right) - \cos\left(x\Gamma t\right)\right], \end{aligned} \tag{2.75}$$

where $x := \frac{\Delta M}{\Gamma}$ and $y := \frac{\Delta\Gamma}{2\Gamma}$ are dimensionless parameters characterising the mixing of neutral mesons. In the case of a mass difference $\Delta M \neq 0$, the mixing is a consequence of $P^0 \leftrightarrow \bar{P}^0$ transitions. The case of a decay width difference $\Delta\Gamma \neq 0$ is equivalent to a difference in the lifetimes of the mass eigenstates and the mixing is a consequence of the disappearance of the shorter-lived eigenstate over time. Since the longer-lived eigenstate is a linear combination of P^0 and $\bar{P}^0$ states, an initially pure P^0 sample acquires a $\bar{P}^0$ component over time.

K^0-$\bar{K}^0$, D^0-$\bar{D}^0$, B^0-$\bar{B}^0$ and B_s^0-$\bar{B}_s^0$ oscillations have all been observed experimentally [23–25]. The current experimental status of the mixing parameters is summarised in Table 2.1 and the corresponding time-dependent mixing probabilities are shown in Fig. 2.4.

The K^0-$\bar{K}^0$ system is characterised by a large difference in lifetimes. The decay of the almost CP-odd K_L^0 to the CP-even $\pi\pi$ final-state is suppressed by $\mathcal{O}\left(10^{-3}\right)$. Additionally, since $M_{\pi\pi\pi} \approx M_{K^0}$, the decay to $\pi\pi\pi$ is kinematically suppressed and as a consequence K_L^0 mesons have a much larger lifetime than K_S^0 mesons.

Table 2.1 Summary of properties and mixing parameters of K^0, D^0, B^0 and B_s^0 mesons at current experimental status [23–25]

	K^0	D^0	B^0	B_s^0
Mean mass M (MeV/c^2)	497	1865	5279	5366
Mass difference ΔM ($\frac{\hbar}{\text{ps}}$)	$(5.27 \pm 0.03) \times 10^{-3}$	$\left(25^{+5.9}_{-6.3}\right) \times 10^{-3}$	0.504 ± 0.004	17.77 ± 0.12
Lifetime τ_H (ps)	51160 ± 210	0.410 ± 0.002	1.519 ± 0.001	1.543 ± 0.060
τ_L (ps)	89.58 ± 0.05	0.410 ± 0.002	1.519 ± 0.001	1.408 ± 0.033
$x = \frac{\Delta M}{\Gamma}$	0.946	0.01	0.776	26.1
$y = \frac{\Delta\Gamma}{2\Gamma}$	0.997	0.01	<0.01	0.05

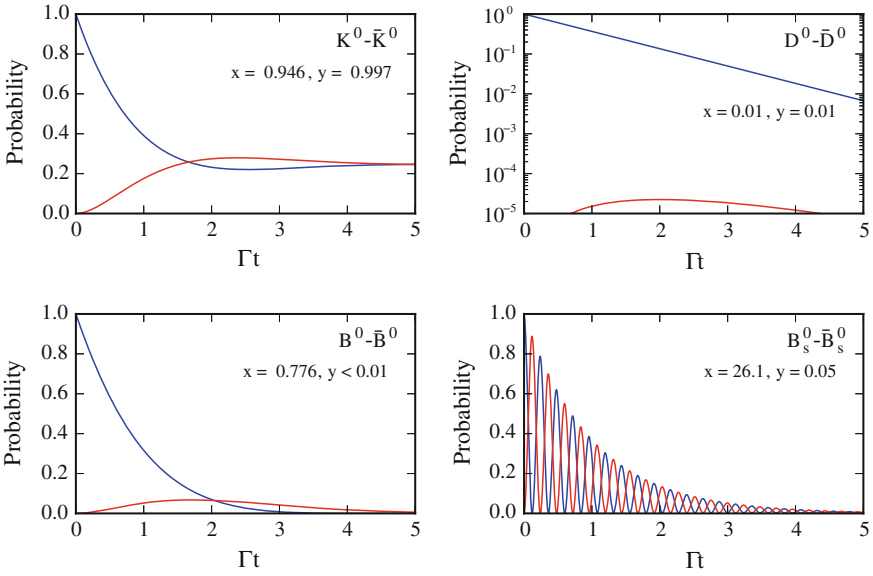

Fig. 2.4 Distributions for the unmixed (*blue*) and mixed (*red*) probabilities in dependence on the proper decay time for initially pure meson samples in the K^0, D^0, B^0 and B_s^0 system. Please note the logarithmic scale for D^0 mesons

Mixing in the D^0-$\bar{D}^0$ system is currently subject of intense experimental and theoretical research. The mixing can proceed via higher order box diagrams of weak interactions or via intermediate states accessible to both D^0 and $\bar{D}^0$ mesons that can have effects on large distances. In the box diagrams, down-type quarks are exchanged and the b-quark contributions, which are due to their large invariant mass typically expected to lead to enhancements, are suppressed by very small CKM matrix elements. The system is described in good approximation by only two generations and therefore GIM-cancellations contribute to further suppressions. As a consequence D^0-$\bar{D}^0$ mixing is a very small effect.

B^0-$\bar{B}^0$ and B_s^0-$\bar{B}_s^0$ oscillations are caused by higher order box diagrams mediated by the exchange of two W bosons and two up-type quarks as shown in Fig. 2.5.

The off-diagonal elements M_{12}^q ($q \in \{d, s\}$) calculated from the box diagrams are given by [26, 27]

$$M_{12}^q = -\frac{G_F^2 M_W^2 \, \eta_B \, M_{B_q} B_{B_q} f_{B_q}^2}{12\pi^2} S_0\left(M_t^2/M_W^2\right)\left(V_{tq}^* V_{tb}\right)^2 e^{i\left(\pi - \phi_{B_q}^{CP}\right)}, \qquad (2.76)$$

where G_F is the Fermi constant, M_i the masses of the B_q mesons and the W bosons, η a perturbative QCD correction, B_{B_q} a non-perturbative parameter related to the involved hadronic matrix element $\langle \bar{B}_q^0 | \left(\bar{b}q\right)_{V-A} \left(b\bar{q}\right)_{V-A} | B_q^0 \rangle$, f_{B_q} the B_q decay con-

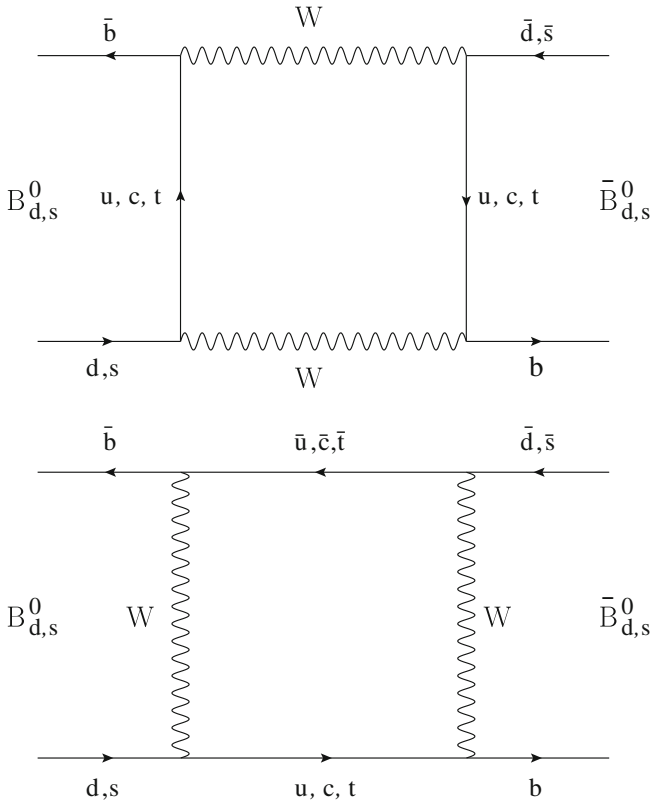

Fig. 2.5 Box diagrams contributing to B^0-$\bar{B}^0$ and B_s^0-$\bar{B}_s^0$ oscillations

stant, $S_0\left(M_t^2/M_W^2\right)$ an Inami-Lin function describing the dependence on the top-quark mass, and $\phi_{B_q}^{CP}$ a convention dependent phase related to CP-transformations of the B flavor eigenstates.

The off-diagonal elements M_{12} are dominated by the contributions of the internal top-quarks. Due to the quadratic dependence on the involved CKM matrix element V_{tq}, the oscillation frequency ΔM is about 35-times higher in the B_s^0-$\bar{B}_s^0$ system with element V_{ts} than in the B^0-$\bar{B}^0$ system with element V_{td}.

M_{12} is related to Γ_{12} by

$$\frac{\Gamma_{12}}{M_{12}} \approx -\frac{3\,\pi}{2S_0\left(M_t^2/M_W^2\right)}\left(\frac{M_b^2}{M_W^2}\right) = \mathcal{O}\left(M_b^2/M_t^2\right) \ll 1 \tag{2.77}$$

The absorptive parts of the Hamiltonian Γ_{12} can give rise to differences in the decay width. The relative decay width differences $\frac{\Delta\Gamma}{\Gamma}$ of the mass eigenstates are given by

$$\frac{\Delta\Gamma}{\Gamma} \approx 16\pi^2 \frac{f_{B_q}^2}{M_{B_q}^2} |V_{cq}|^2. \tag{2.78}$$

In the B^0 system, the decay width difference is very small, $\frac{\Delta\Gamma}{\Gamma} \lesssim \mathcal{O}\left(10^{-2}\right)$, and cannot be resolved at present experiments. In the B_s^0 system, the decay width difference is, with $\frac{\Delta\Gamma}{\Gamma} \approx \mathcal{O}\left(10^{-1}\right)$, sizeable and results in significant different lifetimes of the mass eigenstates, which has been observed experimentally.

Comparing Eqs. 2.52 and 2.76, one finds that the phase of $\frac{q}{p}$ is given by the phase of

$$M_{12}^q = \left|M_{12}^q\right| e^{i\phi_M^q} \quad \text{with} \quad \phi_M^q = \pi + 2\arg\left(V_{tq}^* V_{tb}\right) - \phi_{B_q}^{CP} = 2\beta_{(s)}\,, \tag{2.79}$$

where the convention dependent phase is set to $\phi_{B_q}^{CP} = \pi$. The phases of $\frac{q}{p}$ are directly related to the angle β_s for B_s^0 mesons and to the angle β of the Unitarity Triangle for B^0 mesons. The latter is, being approximately 21°, relatively large.

2.4 CP Violation in Meson Decays

As described in Sects. 2.1 and 2.2, the effect of CP violation in the Standard Model of electroweak interactions is caused by a single irreducible complex phase in the CKM matrix. In weak decays of charged and neutral mesons, CP violation can manifest itself in three different categories: in the decay, in the mixing, and in the interference between mixing and decay. The three categories of CP violation are illustrated in Fig. 2.6 and described in the following.

2.4.1 CP Violation in the Decay

If the magnitudes of the amplitudes of CP-conjugated processes are different, equivalent to

$$\left|\bar{A}_{\bar{f}}/A_f\right| \neq 1, \tag{2.80}$$

then CP violation can occur in the decay. This category of CP violation is referred to as direct CP violation and is the only source of CP violation in decays of charged mesons. This category is illustrated in Fig. 2.6(a).

A necessary condition needed to be satisfied for direct CP violation to emerge is the existence of at least two contributing decay amplitudes with non-vanishing relative weak and strong phases. The weak phases originate from complex CKM matrix elements and enter with opposite sign in A_f and $\bar{A}_{\bar{f}}$. The strong phases originate from hadronic effects, e.g. from rescattering of intermediate on-shell states. The strong

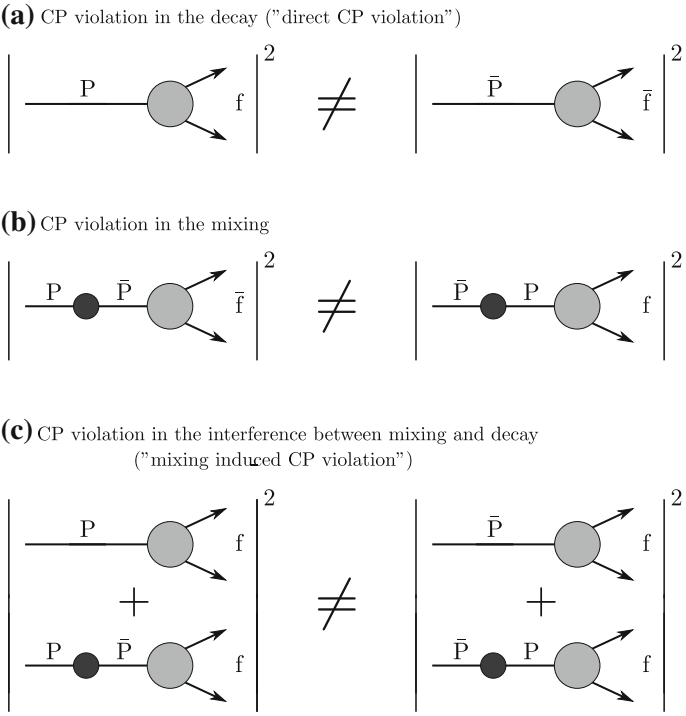

Fig. 2.6 Three categories of CP violation in meson decays. The illustration has been adapted from Ref. [11]

phases need to be different for the amplitudes contributing to the decay. Because strong interactions are invariant under CP-transformations, the strong phases are the same for A_f and $\bar{A}_{\bar{f}}$.

The total amplitude of a decay and of its CP-conjugated decay can be written as

$$A_f = \sum_j \left|a_j\right| e^{i\left(\delta_j + \phi_j\right)} \tag{2.81}$$

$$\text{and} \quad \bar{A}_{\bar{f}} = \sum_j \left|a_j\right| e^{i\left(\delta_j - \phi_j\right)}, \tag{2.82}$$

where a_j denotes single contributing amplitudes, and δ_j and ϕ_j are the associated strong and weak phases. The necessary condition for direct CP violation becomes apparent in the difference of the squared amplitudes,

$$\left|A_f\right|^2 - \left|\bar{A}_{\bar{f}}\right|^2 = 2 \sum_{i,j} \left|a_i\right| \left|a_j\right| \sin\left(\delta_i - \delta_j\right) \sin\left(\phi_i - \phi_j\right). \tag{2.83}$$

Due to the interference, a non-vanishing value in the difference only exists, if the contributing amplitudes provide both: a non-trivial strong phase difference $\delta_i - \delta_j$ and a non-trivial weak phase difference $\phi_i - \phi_j$.

For direct CP violation, an asymmetry can be defined by

$$A_{CP} = \frac{\Gamma\left(P \to f\right) - \Gamma\left(\bar{P} \to \bar{f}\right)}{\Gamma\left(P \to f\right) + \Gamma\left(\bar{P} \to \bar{f}\right)} = \frac{1 - \left|\bar{A}_{\bar{f}}/A_f\right|^2}{1 + \left|\bar{A}_{\bar{f}}/A_f\right|^2} \propto \sin\left(\delta_i - \delta_j\right) \sin\left(\phi_i - \phi_j\right). \tag{2.84}$$

2.4.2 CP Violation in the Mixing

If the complex coefficients q and p differ by more than a phase, equivalent to

$$\left|q/p\right| \neq 1, \tag{2.85}$$

then CP violation occurs in the mixing. This category of CP violation is illustrated in Fig. 2.6(b).

Consider flavor-specific decays satisfying

$$P^0 \to f \nleftarrow \bar{P}^0 \quad \text{and} \quad P^0 \nrightarrow \bar{f} \leftarrow \bar{P}^0, \tag{2.86}$$

equivalent to $|\bar{A}_f| = |A_{\bar{f}}| = 0$, and assume no direct CP violation by requiring $|A_f| = |\bar{A}_{\bar{f}}|$, then the forbidden $\bar{P}^0 \to f$ and $P^0 \to \bar{f}$ decays are only possible due to P^0-$\bar{P}^0$ oscillations. The asymmetry of the forbidden decays calculated from the time-dependent decay rates in Eqs. 2.71 and 2.72 can be expressed as

$$A_{fs} = \frac{\Gamma\left(\bar{P}^0\,(t) \to f\right) - \Gamma\left(P^0\,(t) \to \bar{f}\right)}{\Gamma\left(\bar{P}^0\,(t) \to f\right) + \Gamma\left(P^0\,(t) \to \bar{f}\right)} = \frac{1 - |q/p|^4}{1 + |q/p|^4}, \tag{2.87}$$

and is independent of time. A deviation of the asymmetry from zero and consequently a CP violation in the mixing corresponds to unequal mixing probabilities

$$|\langle \bar{P}^0 | P\,(t)\rangle|^2 \neq |\langle P^0 | \bar{P}\,(t)\rangle|^2. \tag{2.88}$$

2.4.3 CP Violation in the Interference Between Mixing and Decay

In decays to final-states f that are common to P^0 and $\bar{P}^0$, an interference between the decay without mixing, $P^0 \to f$, and the decay with mixing, $P^0 \to \bar{P}^0 \to f$, arises.

CP violation in the interference between mixing and decay occurs, if

$$\mathrm{Im}\,(\lambda_f) \neq 0 \qquad \text{with } \lambda_f = \frac{q}{p}\frac{\bar{A}_f}{A_f}. \tag{2.89}$$

This category of CP violation is referred to as mixing-induced CP violation and is illustrated in Fig. 2.6(c). Mixing-induced CP violation can be observed by the time-dependent asymmetry $A_{CP}\,(t)$ of neutral mesons decaying into CP eigenstates f_{CP}, defined by

$$A_{CP}\,(t) = \frac{\Gamma\left(\bar{P}^0\,(t) \to f_{CP}\right) - \Gamma\left(P^0\,(t) \to f_{CP}\right)}{\Gamma\left(\bar{P}^0\,(t) \to f_{CP}\right) + \Gamma\left(P^0\,(t) \to f_{CP}\right)}. \tag{2.90}$$

The asymmetry calculated from the time-dependent decay rates in Eqs. 2.70 and 2.71 can be expressed as

$$A_{CP}\,(t) = \frac{\mathcal{S}_{CP}^{mix}\sin\,(\Delta M t) - \mathcal{C}_{CP}^{dir}\cos\,(\Delta M t)}{\cosh\,(\Delta\Gamma t/2) - \mathcal{A}_{\Delta\Gamma}\sinh\,(\Delta\Gamma t/2)}, \tag{2.91}$$

where

$$\mathcal{S}_{CP}^{mix} := \frac{2\mathrm{Im}\left(\lambda_{f_{CP}}\right)}{1+\left|\lambda_{f_{CP}}\right|^2}, \qquad \mathcal{C}_{CP}^{dir} := \frac{1-\left|\lambda_{f_{CP}}\right|^2}{1+\left|\lambda_{f_{CP}}\right|^2}, \qquad \mathcal{A}_{\Delta\Gamma} := \frac{2\,\mathrm{Re}\left(\lambda_{f_{CP}}\right)}{1+\left|\lambda_{f_{CP}}\right|^2}, \tag{2.92}$$

$$\text{and} \quad \left|\mathcal{S}_{CP}^{mix}\right|^2 + \left|\mathcal{C}_{CP}^{dir}\right|^2 + |\mathcal{A}_{\Delta\Gamma}|^2 = 1. \tag{2.93}$$

The parameters $\mathcal{S}_{CP}^{mix}$ and $\mathcal{C}_{CP}^{dir}$ measure mixing-induced and direct CP violation, respectively. The parameter $\mathcal{A}_{\Delta\Gamma}$ provides another observable in neutral meson systems with sizeable decay width difference $\Delta\Gamma$.

In the B^0 system, the decay width difference $\Delta\Gamma$ is negligible and the time-dependent CP asymmetry $A_{CP}\,(t)$ in Eq. 2.91 can be rewritten as

$$A_{CP}\,(t) = \mathcal{S}_{CP}^{mix}\sin\,(\Delta M t) - \mathcal{C}_{CP}^{dir}\cos\,(\Delta M t)\,. \tag{2.94}$$

The parameters $\mathcal{S}_{CP}^{mix}$ and $\mathcal{C}_{CP}^{dir}$ are experimentally accessible from the amplitudes of the sine and cosine oscillations in the proper decay times of flavor-tagged decays, see Sect. 2.5. If the amplitudes contributing to a decay all carry the same weak phase, then $|\mathcal{A}_{f_{CP}}| = |\bar{\mathcal{A}}_{f_{CP}}|$ and $|\lambda_{f_{CP}}| = 1$. As a consequence, no direct CP violation occurs and the mixing-induced CP violation,

$$\mathcal{S}_{CP}^{mix} = \mathrm{Im}(\lambda_f), \tag{2.95}$$

is directly related to the phases of the CKM matrix elements involved in the mixing. These decays are referred to as golden modes. Because of its importance, the CP violation in $b \to c\bar{c}s$ transitions in the golden mode of $B^0 \to J/\Psi K_S^0$ decays is discussed in Sect. 2.6.

The objective of the present analysis is the measurement of time-dependent CP violation in $B^0 \to D^+D^-$ and $B^0 \to D^{*\pm}D^{\mp}$ decays. These decays are mediated by $b \to c\bar{c}d$ transitions. As it will be discussed in Sect. 2.7, $b \to d$ penguin amplitudes that may have different weak phases can contribute to the decays and possibly result in $|\lambda_{f_{CP}}| \neq 1$. Consequently, in addition to mixing-induced CP violation that is expected to be similar to that in $b \to c\bar{c}s$ transitions, the penguin amplitudes might give rise to direct CP violation.

2.5 Coherent $B^0\bar{B}^0$ Mixing

At the Belle experiment, B mesons are produced by the asymmetric-energy e^+e^--collider KEKB via the decay of the $\Upsilon(4S)$-resonance. Neutral $B\bar{B}$ mesons originating from $\Upsilon(4S)$ decays are produced in an entangled quantum state and evolve coherently. The decay flavor of one of the B mesons determines the flavor content of the second B meson to be opposite at this particular instant of time. This is a manifestation of the Einstein-Podolsky-Rosen (EPR) effect [28] and is important for the time-dependent CP violation measurements at the Belle experiment.

Starting from the two-body wave function describing the entangled $B^0\bar{B}^0$ state and applying the theory of the time evolution of neutral mesons from Sect. 2.3, the rate of the joint decay of both B mesons, the resulting CP asymmetries and the probability distributions needed for the time-dependent CP violation measurements in the present analysis are derived.

The mechanism of coherent $B\bar{B}$ pair production via decays of the $\Upsilon(4S)$-resonance is shown in Fig. 2.7. The $\Upsilon(4S)$ has the quantum numbers $J^{PC} = 1^{--}$. The decay of the $\Upsilon(4S)$ into $B\bar{B}$ pairs is a strong interaction process that conserves the quantum

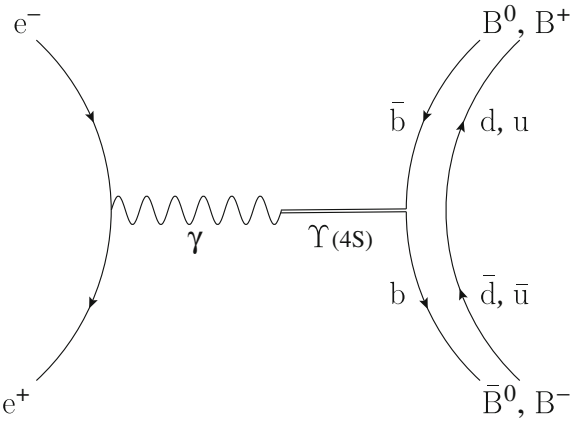

Fig. 2.7 Illustration of the mechanism of coherent $B\bar{B}$ pair production via the $\Upsilon(4S)$-resonance at e^+e^--colliders

numbers. B mesons are pseudo-scalars and the $B^0\bar{B}^0$ state is produced with orbital angular momentum $L = 1$ in a P-wave configuration. The parity of the system is $P = (-1)^L = -1$ and requires the spatial part of the wave function of the $B^0\bar{B}^0$ state to be antisymmetric. The Bose-Einstein statistics requires the overall wave function to be symmetric. Consequently, the flavor part of the wave function, denoted in the following by Ψ, needs also to be antisymmetric and can be written as

$$|\Psi(t_1, t_2)\rangle = \frac{1}{\sqrt{2}}\left(|B^0(t_1)\rangle|\bar{B}^0(t_2)\rangle - |\bar{B}^0(t_1)\rangle|B^0(t_2)\rangle\right). \tag{2.96}$$

Consider one of the B mesons decays at time t_1 to the final-state f_a and assume the second B meson decays at time t_2 to the final-state f_b, then the joint amplitude can be expressed as

$$\langle f_a f_b|\Psi(t_1, t_2)\rangle = \frac{1}{\sqrt{2}}\left(\langle f_a|B^0(t_1)\rangle\langle f_b|\bar{B}^0(t_2)\rangle - \langle f_a|\bar{B}^0(t_1)\rangle\langle f_b|B^0(t_2)\rangle\right). \tag{2.97}$$

By defining the amplitudes

$$A_i := \langle f_i|B^0\rangle \quad \text{and} \quad \bar{A}_i := \langle f_i|\bar{B}^0\rangle, \tag{2.98}$$

and introducing the time evolution of the flavor eigenstates from Eqs. 2.58 and 2.59, the joint amplitude can be written as

$$\begin{aligned}\langle f_a f_b|\Psi(t_1, t_2)\rangle = \frac{1}{\sqrt{2}}\Big\{&\Big[g_+(t_1)g_+(t_2) - g_-(t_1)g_-(t_2)\Big]\Big(A_a\bar{A}_b - \bar{A}_a A_b\Big)\\ &+ \Big[g_+(t_1)g_-(t_2) - g_-(t_1)g_+(t_2)\Big]\Big(\frac{p}{q}A_a A_b - \frac{q}{p}\bar{A}_a\bar{A}_b\Big)\Big\}.\end{aligned} \tag{2.99}$$

The time-dependent decay rate is obtained from the absolute square of the joint amplitude. By substituting the functions $g_+(t)$ and $g_-(t)$ defined in Eqs. 2.60 and 2.61, the decay rate is given by [29]

$$\begin{aligned}&\Gamma\left[\Psi(t_1, t_2) \to f_a f_b\right] = \left|\langle f_a f_b|\Psi(t_1, t_2)\rangle\right|^2\\ &= \frac{1}{2}e^{-\Gamma(t_1+t_2)}\Big\{\Big(|A_a|^2 + |\bar{A}_a|^2\Big)\Big(|A_b|^2 + |\bar{A}_b|^2\Big) - 4\,\mathrm{Re}\Big(\frac{q}{p}A_a^*\bar{A}_a\Big)\mathrm{Re}\Big(\frac{q}{p}A_b^*\bar{A}_b\Big)\\ &\quad - 2\sin\left[\Delta M(t_1 - t_2)\right]\Big[\mathrm{Im}\Big(\frac{q}{p}A_a^*\bar{A}_a\Big)\Big(|A_b|^2 - |\bar{A}_b|^2\Big) - \Big(|A_a|^2 - |\bar{A}_a|^2\Big)\mathrm{Im}\Big(\frac{q}{p}A_b^*\bar{A}_b\Big)\Big]\\ &\quad - \cos\left[\Delta M(t_1 - t_2)\right]\Big[\Big(|A_a|^2 - |\bar{A}_a|^2\Big)\Big(|A_b|^2 - |\bar{A}_b|^2\Big) + 4\,\mathrm{Im}\Big(\frac{q}{p}A_a^*\bar{A}_a\Big)\mathrm{Im}\Big(\frac{q}{p}A_b^*\bar{A}_b\Big)\Big]\Big\}.\end{aligned} \tag{2.100}$$

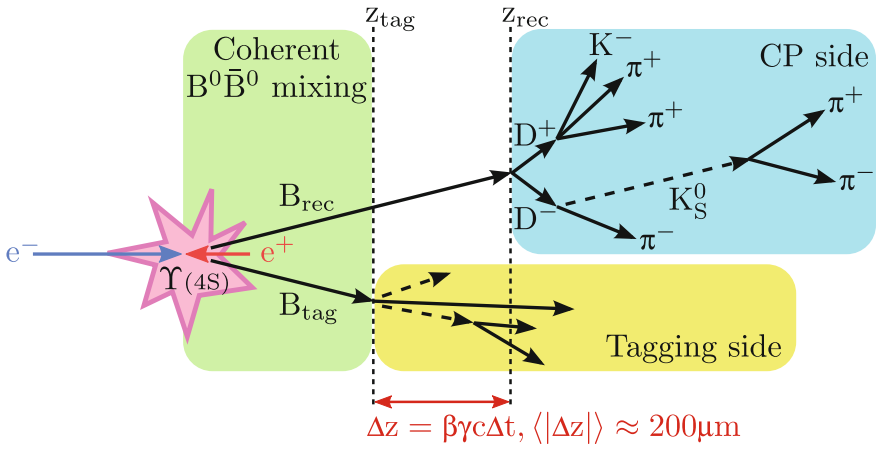

Fig. 2.8 Principle of time-dependent CP violation measurements at the Belle experiment: Due to the asymmetric-energy of the e^+e^--collider, the $B^0\bar{B}^0$ pairs from $\Upsilon(4S)$ decays are produced with a Lorentz boost along the e^--beam. The neutral B mesons evolve coherently, until one B meson decays and determines by an EPR-like correlation the flavor content of the second B meson to be opposite. The second B meson then oscillates independently and decays. In the time-dependent CP violation measurements, one B meson is reconstructed in a CP eigenstate, e.g. in $B^0 \to D^+D^-$, and the flavor of the other B meson is determined from its decay products. The measurements of the displaced decay vertices of the B mesons allow to translate the flight length difference Δz into a proper decay time difference Δt. The combination of the flavor information of the second B meson with the Δt measurement enables to measure the time-dependent CP violating asymmetry given by Eq. 2.103

Equation 2.100 describes the time-dependent decay rate of an entangled $B^0\bar{B}^0$ pair produced by the $\Upsilon(4S)$-resonance and decaying to the final-states f_a and f_b. Assuming CPT invariance and no CP violation in the mixing equivalent to $|q/p| = 1$, the decay rate can be used to calculate the time-dependence of any neutral weak decay process.

The dynamics in the time evolution depends on the proper decay time difference of both B mesons, $t_1 - t_2$, and not on their sum, $t_1 + t_2$. This dependence is already implicitly included in the decay rates in the classic paper by I.I. Bigi and A.I. Sanda [30], predicting CP violation in the B meson system in 1987 (see the emphasised minus signs in Eq. 2.6 in Fig. 1.1(b)) and is the reason for the asymmetry in the energy of the beams at the e^+e^--collider KEKB. The asymmetry causes a Lorentz boost of the $\Upsilon(4S)$, and thereby increases the spatial separation of the B meson decay vertices. The translation of measurements of the decay flight length differences with the known Lorentz boost into proper decay time differences allows to observe time-dependent CP violation in the B meson system. The principle of the time-dependent CP violation measurements is illustrated in Fig. 2.8.

Consider one of the neutral B mesons decays at time t_{CP} to a CP eigenstate f_{CP}, for example $B^0 \to D^+D^-$. Assuming the second B meson decays at time t_{tag} flavor-specific as a B^0 to f_{tag}, corresponding to $A_{tag} := A_b = \langle f_{tag}|B^0\rangle$ and $\bar{A}_b = 0$. By introducing $\lambda_{f_{CP}}$ defined in Eq. 2.69, the time-dependent decay rate can be written as

$$\Gamma\left[\Psi\left(t_{CP}, t_{tag}\right) \to f_{CP} f_{tag}\right] = \left|\langle f_{CP} f_{tag} | \Psi\left(t_{CP}, t_{tag}\right)\rangle\right|^2$$
$$= \frac{1}{2} e^{-\Gamma\left(t_{CP}+t_{tag}\right)} \left|A_{CP}\right|^2 \left|A_{tag}\right|^2 \left[\left(1 + \left|\lambda_{f_{CP}}\right|^2\right)\right.$$
$$\left. - 2\,\mathrm{Im}\left(\lambda_{f_{CP}}\right) \sin\left[\left(\Delta M\left(t_{CP} - t_{tag}\right)\right] - \left(1 - \left|\lambda_{f_{CP}}\right|^2\right) \cos\left[\left(\Delta M\left(t_{CP} - t_{tag}\right)\right]\right]. \tag{2.101}$$

In the opposite case, if the second B meson decays at time t_{tag} flavor-specific as a $\bar{B}^0$ to $\bar{f}_{tag}$, corresponding to $A_{tag} := \bar{A}_b = \langle \bar{f}_{tag} | \bar{B}^0 \rangle$ and $A_b = 0$, then the time-dependent decay rate can be written as

$$\Gamma\left[\Psi\left(t_{CP}, t_{tag}\right) \to f_{CP} \bar{f}_{tag}\right] = \left|\langle f_{CP} \bar{f}_{tag} | \Psi\left(t_{CP}, t_{tag}\right)\rangle\right|^2$$
$$= \frac{1}{2} e^{-\Gamma\left(t_{CP}+t_{tag}\right)} \left|A_{CP}\right|^2 \left|A_{tag}\right|^2 \left[\left(1 + \left|\lambda_{f_{CP}}\right|^2\right)\right.$$
$$\left. + 2\,\mathrm{Im}\left(\lambda_{f_{CP}}\right) \sin\left[\left(\Delta M\left(t_{CP} - t_{tag}\right)\right] + \left(1 - \left|\lambda_{f_{CP}}\right|^2\right) \cos\left[\left(\Delta M\left(t_{CP} - t_{tag}\right)\right]\right]. \tag{2.102}$$

Again in the decay rates the time-dependence of the dynamics originates from the proper decay time differences, denoted in the following by $\Delta t = t_{CP} - t_{tag}$. The sine and cosine oscillations in the decay rates have opposite signs depending on whether the second B meson, referred to as B_{tag}, decays as a B^0 or as a $\bar{B}^0$. Furthermore, the amplitudes of the sine and cosine oscillations provide observables sensitive to mixing-induced and direct CP violation according to the definitions in Eq. 2.92.

The time-dependent CP asymmetry $A_{CP}(t)$ constructed from the time-dependent decay rates in Eqs. 2.101 and 2.102 is

$$A_{CP}(\Delta t) = \frac{\Gamma\left[\Psi\left(t_{CP}, t_{tag}\right) \to f_{CP} \bar{f}_{tag}\right] - \Gamma\left[\Psi\left(t_{CP}, t_{tag}\right) \to f_{CP} f_{tag}\right]}{\Gamma\left[\Psi\left(t_{CP}, t_{tag}\right) \to f_{CP} \bar{f}_{tag}\right] + \Gamma\left[\Psi\left(t_{CP}, t_{tag}\right) \to f_{CP} f_{tag}\right]}$$
$$= \mathcal{S}_{CP}^{mix} \sin\left(\Delta M \Delta t\right) - \mathcal{C}_{CP}^{dir} \cos\left(\Delta M \Delta t\right). \tag{2.103}$$

Compared to the time-dependent CP asymmetry introduced in Eq. 2.94, one finds, that $A_{CP}(t)$ has the same form, but depends on the proper decay time difference Δt of two B mesons in an $\Upsilon(4S)$ event instead of the proper decay time of one B meson.

By integration over the experimentally not accessible sum of proper decay times, $t_{CP} + t_{tag}$, and by normalisation to the possible proper decay time difference interval of $-\infty < \Delta t < +\infty$, in an $\Upsilon(4S)$ event the probability to find one B meson decaying to a CP eigenstate and the second B meson decaying flavor-specific with a proper decay time difference Δt is

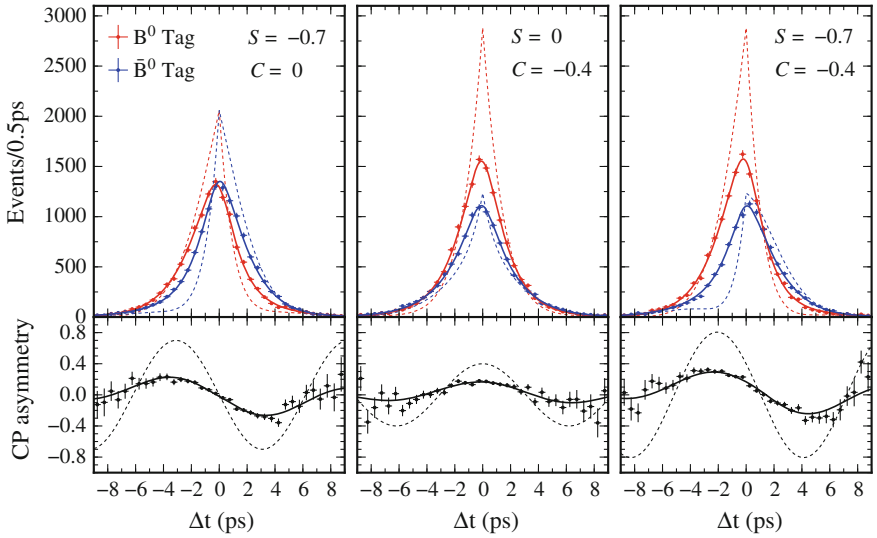

Fig. 2.9 Theoretical (*dashed lines*) and experimental (*solid lines*) proper decay time difference distributions and the corresponding CP asymmetries for three different scenarios of mixing-induced CP violation $\mathcal{S}$ and direct CP violation $\mathcal{C}$

$$P(\Delta t, q) = \frac{1}{4\tau_{B^0}} e^{-|\Delta t|/\tau_{B^0}} \left[1 + q\left(\mathcal{S}_{CP}^{mix} \sin(\Delta m \Delta t) - \mathcal{C}_{CP}^{dir} \cos(\Delta m \Delta t)\right)\right], \tag{2.104}$$

where $q = +1$ (-1) represents the b-flavor charge, when the second B meson is tagged as B^0 ($\bar{B}^0$).

In Fig. 2.9 the distributions for B^0 and $\bar{B}^0$ tags and the corresponding CP asymmetries for three different scenarios of CP violation are shown.

- In the first scenario, a non-vanishing mixing-induced CP violation ($\mathcal{S} \neq 0$) with no direct CP violation ($\mathcal{C} = 0$) shifts and deforms the Δt distributions for B^0 (red) and $\bar{B}^0$ (blue) tags horizontally. The resulting time-dependent CP asymmetry follows a sine oscillation.
- In the second scenario, a non-vanishing direct CP violation ($\mathcal{C} \neq 0$) with no mixing-induced CP violation ($\mathcal{S} = 0$) shifts the Δt distributions vertically. The direct CP violation causes one decay to occur more or less frequently than that of its CP-conjugated process. The resulting CP asymmetry follows a cosine oscillation.
- In the third scenario, a non-vanishing mixing-induced and a non-vanishing direct CP violation, ($\mathcal{S} \neq 0$ and $\mathcal{C} \neq 0$) are present. The Δt distributions are shifted and deformed both, horizontally and vertically, and the resulting CP asymmetry is a superposition of sine and cosine oscillations.

The CP violation measurements are performed at the Belle experiment as illustrated in Fig. 2.8. One experimental difficulty is to resolve the proper decay time differences. Due to the low Lorentz boost, the resolution in the measurements of the decay flight length difference of the two B mesons is in the same order as the average

flight length difference. The effect of the resolution is visible when comparing the theoretical (dashed lines) and experimental (solid lines) Δt distributions in Fig. 2.9. In addition, the experimental assignment of the flavor of the B_{tag} meson from its decay products cannot be perfect. The uncertainties in the flavor tagging decision and possible mistags affect the measurement of the sine and cosine time-dependence and effectively result in a reduction of the measured amplitudes. This effect is visible in the time-dependent CP asymmetries in Fig. 2.9: the amplitudes of the experimental oscillations are lower than the theoretical ones.

2.6 CP Violation in $b \to c\bar{c}s$ Transitions

In the B meson system CP violation has been observed for the first time in $b \to c\bar{c}s$ transitions such as in $B^0 \to J/\Psi K_S^0$ decays [31, 32]. This decay is referred to as the golden mode for the determination of the angle β of the Unitarity Triangle and is discussed in the following.

In $B^0 \to J/\Psi K_S^0$ decays the J/Ψ and the K_S^0 are produced with orbital angular momentum of $L = 1$ in a P-wave configuration. Neglecting the small CP violation in K^0-$\bar{K}^0$ mixing, the K_S^0 has like the J/Ψ a CP eigenvalue of $+1$. In combination with the $(-1)^{L=1} = -1$ contribution from the angular momentum, the $J/\Psi K_S^0$ final-state has the CP eigenvalue $\eta_{CP} = -1$.

The tree-level and penguin diagrams contributing to $B^0 \to J/\Psi K_S^0$ decays are shown in Fig. 2.10. On tree-level, the decay is mediated by $b \to c\bar{c}s$ transitions that are color-suppressed due to the internal emission of a W boson. The penguin diagrams have an internal loop with virtual up-type quarks. The loops involving virtual $\bar{c}$ and $\bar{t}$ quarks have CKM matrix elements of the same order as the transitions in the tree diagram and carry the same weak phase. In contrast, the loop involving virtual $\bar{u}$ quarks, that could introduce a different weak phase via V_{ub}, is suppressed by a factor of λ^2, where $\lambda \approx 0.23$ refers to the expansion parameter in the Wolfenstein parameterisation. In the penguin diagrams, the $c\bar{c}$ pair forming the J/Ψ is created from gluons. Since the $c\bar{c}$ pair has to be created in a color singlet state, it cannot be created from a single gluon. All above effects result in a high suppression of the penguin amplitudes. No so-called penguin pollution and hence no direct CP violation are expected to emerge in $b \to c\bar{c}s$ transitions.

The mixing-induced CP violation in $B^0 \to J/\Psi K_S^0$ decays can be estimated from the involved decay amplitudes and mixing-phases. The parameter $\lambda_{J/\Psi K_S^0}$ defined in Eq. 2.69 characterises the mixing-induced CP violation explained in Sect. 2.4.3. It depends on the ratio q/p which introduces the B mixing phase and the amplitudes of the CP-conjugated decays. Since B^0 mesons decay to $J/\Psi K^0$, but $\bar{B}^0$ mesons decay to $J/\Psi \bar{K}^0$, the $J/\Psi K_S^0$ final-state involves K^0-$\bar{K}^0$ mixing and $\lambda_{J/\Psi K_S^0}$ includes also the neutral kaon mixing phase. The parameter $\lambda_{J/\Psi K_S^0}$ can then be expressed as

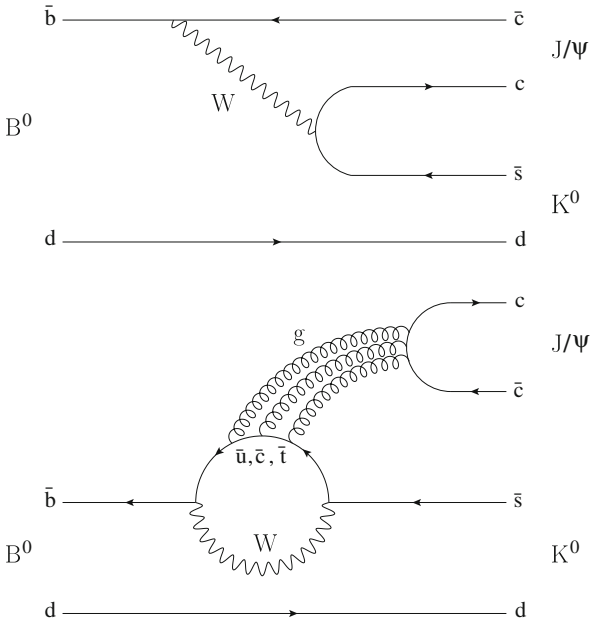

Fig. 2.10 Tree-level (*top*) and penguin diagrams (*bottom*) contributing to $B^0 \to J/\Psi K^0_{S,L}$ decays

$$\begin{aligned}\lambda_{J/\Psi K^0_S} &= \left(\frac{q}{p}\right)_{B^0} \frac{\bar{A}}{A} \left(\frac{q}{p}\right)_{K^0} \\ &= \eta_{CP} \frac{V^*_{tb} V_{td}}{V_{tb} V^*_{td}} \frac{V_{cb} V^*_{cs}}{V^*_{cb} V_{cs}} \frac{V^*_{cd} V_{cs}}{V_{cd} V^*_{cs}} \\ &= \eta_{CP} e^{-2i\beta}, \end{aligned} \tag{2.105}$$

where β refers to the angle of the Unitarity Triangle defined in Eq. 2.45.

Because of $\mathcal{S}^{mix}_{J/\Psi K^0_S} = -\eta_{CP} \sin(2\beta)$, the resulting time-dependent CP asymmetry in $B^0 \to J/\Psi K^0_S$ decays is

$$A_{CP}(\Delta t) = -\eta_{CP} \sin(2\beta) \sin(\Delta M \Delta t). \tag{2.106}$$

Thus the angle β of the Unitarity Triangle can be determined by time-dependent CP asymmetry measurements of $B^0 \to J/\Psi K^0_S$ decays. The same arguments also hold for other $b \to c\bar{c}s$ transitions, for example $B^0 \to J/\Psi K^0_L$ decays with $\eta_{CP} = +1$.

The current world average of $\sin(2\beta)$ from $b \to c\bar{c}s$ transitions is

$$\sin(2\beta) = 0.68 \pm 0.02, \tag{2.107}$$

which corresponds to a value of $\beta = (21.4 \pm 0.8)^\circ$ [33]. Due to the high precision in $b \to c\bar{c}s$ transitions achieved by the B-factory experiments BaBar and Belle, the sin (2β) result provides a Standard Model reference and contributes to put tight constraints on the CKM metrology, e.g. on the Unitarity Triangle shown in Fig. 2.3.

2.7 CP Violation in b → cc̄d Transitions

The Feynman diagrams contributing to $B^0 \to D^+D^-$, $D^{*+}D^-$, $D^{*-}D^+$ and $D^{*+}D^{*-}$ decays, referred to as neutral B meson to double-charm decays, are shown in Fig. 2.11. On tree level, the decays are mediated by Cabibbo-disfavored, but color-allowed $b \to c\bar{c}d$ transitions. In addition to the tree-level diagrams, $b \to d$ penguin diagrams can contribute to the decays. The CKM matrix elements of the penguin amplitudes are of same order of magnitude as the elements of the tree-level amplitudes, but can carry different weak phases.

In contrast to $B^0 \to D^+D^-$, $D^{*+}D^-$ and $D^{*-}D^+$ decays, $B^0 \to D^{*+}D^{*-}$ is the decay of a pseudo-scalar meson to two vector mesons and involves a mixing of CP-even and CP-odd states which can be disentangled by an angular analysis. The measurements of $B^0 \to D^{*+}D^{*-}$ decays are not part of this work and have been carried out in parallel by the Belle Collaboration [34, 35]. The present analysis covers the measurement of branching fractions and time-dependent CP violation in $B^0 \to D^+D^-$, $D^{*+}D^-$ and $D^{*-}D^+$ decays. These decays are discussed in the following.

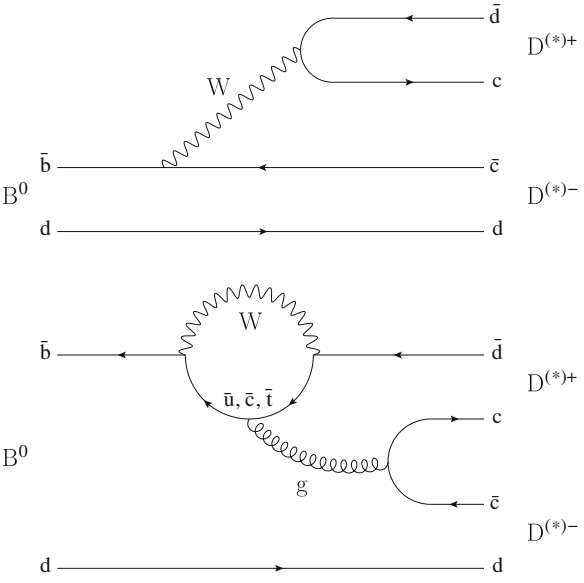

Fig. 2.11 Tree-level (*top*) and penguin diagrams (*bottom*) contributing to $B^0 \to D^{(*)+}D^{(*)-}$ decays

2.7.1 CP Violation in $B^0 \to D^+D^-$ Decays

The D^+D^- configuration is a CP eigenstate with eigenvalue $\eta_{CP} = +1$. The total decay amplitude of the $B^0 \to D^+D^-$ decay involves contributions from tree-level amplitudes (A_T) and penguin amplitudes (A_P^q with $q \in \{u, c, t\}$) and can be written as [36, 37]

$$A\left(B^0 \to D^+D^-\right) = \lambda_c^{(d)}\left(A_T + A_P^c\right) + \lambda_u^{(d)} A_P^u + \lambda_t^{(d)} A_P^t, \tag{2.108}$$

where $\lambda_q^{(d)} = V_{qd} V_{qb}^*$.

By introducing the relative strong phase δ and the relative weak phase γ between the decay amplitudes, the total decay amplitudes can be rewritten as

$$A\left(B^0 \to D^+D^-\right) = \mathcal{A}\left[1 - r\, e^{i(\delta+\gamma)}\right], \tag{2.109}$$

$$\bar{A}\left(B^0 \to D^+D^-\right) = \mathcal{A}\left[1 - r\, e^{i(\delta-\gamma)}\right], \tag{2.110}$$

where $\mathcal{A}$ refers to the CP conserving amplitude governed by the tree-level contributions and the ratio r measures the suppression of the penguin amplitudes with respect to the tree amplitude.

According to

$$\lambda_{D^+D^-} = e^{-2i\beta}\, \frac{\bar{A}\left(B^0 \to D^+D^-\right)}{A\left(B^0 \to D^+D^-\right)}, \tag{2.111}$$

the CP violation in $B^0 \to D^+D^-$ decays is determined by the expressions

$$\begin{aligned} \mathcal{S}_{D^+D^-}^{mix} &= \frac{2\,\mathrm{Im}\,(\lambda_{D^+D^-})}{1 + |\lambda_{D^+D^-}|^2} = -\frac{\sin(2\beta) + 2r\cos(\delta)\sin(2\beta+\gamma) + r^2\sin[2(\beta+\gamma)]}{1 + 2r\cos(\delta)\cos(\gamma) + r^2} \\ &\approx -\sin(2\beta) - 2r\cos(2\beta)\cos(\delta)\sin(\gamma)\,, \end{aligned} \tag{2.112}$$

$$\begin{aligned} \mathcal{C}_{D^+D^-}^{dir} &= \frac{1 - |\lambda_{D^+D^-}|^2}{1 + |\lambda_{D^+D^-}|^2} = -\frac{2r\sin(\delta)\sin(\gamma)}{1 + 2r\cos(\delta)\cos(\gamma) + r^2} \\ &\approx -2r\sin(\delta)\sin(\gamma)\,. \end{aligned} \tag{2.113}$$

In the case of negligible penguin contributions, the direct CP violation vanishes and the mixing-induced CP violation in $B^0 \to D^+D^-$ decays is exactly $\mathcal{S}_{D^+D^-}^{mix} = -\sin(2\beta)$. This case is equivalent to the CP violation in the golden modes involving $b \to c\bar{c}s$ transitions such as in $B^0 \to J/\Psi K_S^0$ decays discussed in Sect. 2.6.

In the case of sizeable penguin amplitudes, the mixing-induced CP violation is shifted with respect to $-\sin(2\beta)$ depending on the magnitude of the ratio r. Additionally, in combination with a non-vanishing relative strong phase a non-zero direct CP violation can emerge.

The calculation of the contributions of penguin amplitudes are associated with difficulties due to hadronic effects. The decays involve charm quarks in intermediate and final-states which give rise to long-range interactions. This complicates certain theoretical approaches such as calculations based on factorization approximations. The current theoretical predictions on mixing-induced and direct CP violation in $B^0 \to D^+D^-$ decays are associated with large uncertainties. Standard Model conform model-dependent and model-independent predictions for the ratio r corresponding to the suppression of the penguin contributions range from values as low as 0.03 [38] to upper bounds of 0.3 [39–41]. Even larger contributions can be accommodated in extensions of the Standard Model [42].

CP violation in b → cc̄d transitions has been previously studied by both, the Belle and the BaBar Collaborations. In 2007, Belle using a data set of 535×10^6 $B\bar{B}$ pairs has found evidence of a large direct CP violation in $B^0 \to D^+D^-$ decays: $\mathcal{C}^{\text{dir}}_{D^+D^-} = -0.91 \pm 0.23\ (\text{stat.}) \pm 0.06\ (\text{syst.})$, corresponding to a $3.2\,\sigma$ deviation from zero [43]. This deviation has not been confirmed by BaBar and has not been observed in other $B^0 \to D^{*\pm}D^{(*)\mp}$ decay modes [44–46].

The objective of the present analysis is the measurement of the branching fraction and time-dependent CP violation in $B^0 \to D^+D^-$ decays using the final Belle data set of 772×10^6 $B\bar{B}$ pairs. Furthermore, to provide a comparison to a directly related decay, the analysis covers additionally the measurement of $B^0 \to D^{*\pm}D^{\mp}$ decays.

2.7.2 CP Violation in $B^0 \to D^{*\pm}D^{\mp}$ Decays

The $B^0 \to D^{*\pm}D^{\mp}$ decays allow to probe independently from $B^0 \to D^+D^-$ decays for penguin effects in double-charm decays. Unlike D^+D^-, the $D^{*+}D^-$ and $D^{*-}D^+$ configurations are not CP eigenstates. Both states are accessible from B^0 and $\bar{B}^0$ with decay amplitudes of comparable magnitudes. Therefore an interference between direct decays and decays following B^0-$\bar{B}^0$ oscillations emerges, and effects of mixing-induced and direct CP violation in analogy to those in $B^0 \to D^+D^-$ decays are expected.

The time-dependent decay rate for $B^0 \to D^{*\pm}D^{\mp}$ has four flavor-charge configurations and can be written as

$$\begin{aligned} f_{D^{*\pm}D^{\mp}}(\Delta t) = \left(1 \pm \mathcal{A}_{D^*D}\right) \frac{e^{-|\Delta t|/\tau_{B^0}}}{8\,\tau_{B^0}} \\ \times \left\{1 + q\left[\mathcal{S}_{D^{*\pm}D^{\mp}} \sin\left(\Delta m \Delta t\right) - \mathcal{C}_{D^{*\pm}D^{\mp}} \cos\left(\Delta m \Delta t\right)\right]\right\}. \end{aligned} \tag{2.114}$$

Generally, the parameters $\mathcal{S}_{D^{*\pm}D^{\mp}}$ and $\mathcal{C}_{D^{*\pm}D^{\mp}}$ for the $D^{*+}D^-$ and $D^{*-}D^+$ configurations are not independent, but related by $\mathcal{S}_{D^{*\pm}D^{\mp}} = -\sqrt{1 - \mathcal{C}^2_{D^{*\pm}D^{\mp}}} \sin\left(2\,\beta_{\text{eff}} \pm \delta\right)$ [47]. The expression includes the sensitivity on the angle β, which can be modified

by penguin contributions to the effective angle β_{eff}, and on the relative strong phase δ between the $B^0 \to D^{*+}D^-$ and $B^0 \to D^{*-}D^+$ decay amplitudes.

The time- and flavor-integrated asymmetry $\mathcal{A}_{D^*D}$ is defined by

$$\mathcal{A}_{D^*D} = \frac{N_{D^{*+}D^-} - N_{D^{*-}D^+}}{N_{D^{*+}D^-} + N_{D^{*-}D^+}}, \tag{2.115}$$

and measures direct CP violation in $B^0 \to D^{*\pm}D^{\mp}$ decays.

The decay rate in Eq. 2.114 can be expressed in an equivalent parameterisation given by [48]

$$\begin{aligned}
\mathcal{S}_{D^*D} &= \frac{1}{2}\left(\mathcal{S}_{D^{*+}D^-} + \mathcal{S}_{D^{*-}D^+}\right), \\
\mathcal{C}_{D^*D} &= \frac{1}{2}\left(\mathcal{C}_{D^{*+}D^-} + \mathcal{C}_{D^{*-}D^+}\right), \\
\Delta\mathcal{S}_{D^*D} &= \frac{1}{2}\left(\mathcal{S}_{D^{*+}D^-} - \mathcal{S}_{D^{*-}D^+}\right), \\
\Delta\mathcal{C}_{D^*D} &= \frac{1}{2}\left(\mathcal{C}_{D^{*+}D^-} - \mathcal{C}_{D^{*-}D^+}\right).
\end{aligned} \tag{2.116}$$

In this parameterisation, the decay rate of $B^0 \to D^{*\pm}D^{\mp}$ decays can be written as

$$\begin{aligned}
f_{D^{*\pm}D^{\mp}}(\Delta t) = \left(1 \pm \mathcal{A}_{D^*D}\right)\frac{e^{-|\Delta t|/\tau_{B^0}}}{8\,\tau_{B^0}}\Bigg\{1 + q\Big[\Big(\mathcal{S}_{D^*D} \pm \Delta\mathcal{S}_{D^*D}\Big)\sin\big(\Delta m \Delta t\big) \\
- \Big(\mathcal{C}_{D^*D} \pm \Delta\mathcal{C}_{D^*D}\Big)\cos\big(\Delta m \Delta t\big)\Big]\Bigg\},
\end{aligned} \tag{2.117}$$

where $\mathcal{S}_{D^*D}$ parameterises mixing-induced and $\mathcal{C}_{D^*D}$ flavor-dependent direct CP violation. The parameters $\Delta\mathcal{S}_{D^*D}$ and $\Delta\mathcal{C}_{D^*D}$ are not sensitive to CP violation. The parameter $\Delta\mathcal{S}_{D^*D}$ is related to the relative strong phase δ between the decay amplitudes and $\Delta\mathcal{C}_{D^*D}$ describes the asymmetry between the rates $\Gamma(B^0 \to D^{*+}D^-) + \Gamma(\bar{B}^0 \to D^{*-}D^+)$ and $\Gamma(B^0 \to D^{*-}D^+) + \Gamma(\bar{B}^0 \to D^{*+}D^-)$.

If the contributions of penguin amplitudes to $B^0 \to D^{*\pm}D^{\mp}$ decays are negligible, and the relative strong phase between the $B^0 \to D^{*+}D^-$ and $B^0 \to D^{*-}D^+$ decay amplitudes is zero and their magnitudes are the same, then

$$\mathcal{A}_{D^*D} = 0, \quad \mathcal{S}_{D^{*+}D^-} = \mathcal{S}_{D^{*-}D^+} = -\sin(2\beta), \quad \mathcal{C}_{D^{*+}D^-} = \mathcal{C}_{D^{*-}D^+} = 0, \tag{2.118}$$

or equivalent

$$\mathcal{A}_{D^*D} = 0, \quad \mathcal{S}_{D^*D} = -\sin(2\beta), \quad \mathcal{C}_{D^*D} = \Delta\mathcal{S}_{D^*D} = \Delta\mathcal{C}_{D^*D} = 0. \tag{2.119}$$

In this case, the time-dependent CP violating asymmetry in $B^0 \to D^{*\pm}D^{\mp}$ decays measures directly $-\sin(2\beta)$.

References

1. S.L. Glashow, Partial-symmetries of weak interactions. Nucl. Phys. **22**, 579–588 (1961)
2. S. Weinberg, A model of leptons. Phys. Rev. Lett. **19**, 1264–1266 (1967)
3. P. Higgs, Broken symmetries, massless particles and gauge fields. Phys. Lett. **12**, 132–133 (1964)
4. F. Englert, R. Brout, Broken symmetry and the mass of gauge vector mesons. Phys. Rev. Lett. **13**, 321–323 (1964)
5. G.S. Guralnik, C.R. Hagen, T.W.B. Kibble, Global conservation laws and massless particles. Phys. Rev. Lett. **13**, 585–587 (1964)
6. Y. Nambu, Quasiparticles and gauge invariance in the theory of superconductivity. Phys. Rev. **117**, 648–663 (1960)
7. J. Goldstone, Field theories with superconductor solutions. Il Nuovo Cimento **19**, 154–164 (1961)
8. J. Goldstone, A. Salam, S. Weinberg, Broken symmetries. Phys. Rev. **127**, 965–970 (1962)
9. S.L. Glashow, J. Iliopoulos, L. Maiani, Weak interactions with lepton-hadron symmetry. Phys. Rev. D **2**, 1285–1292 (1970)
10. M. Kobayashi, T. Maskawa, CP violation in the renormalizable theory of weak interaction. Prog. Theor. Phys. **49**, 652–657 (1973)
11. I.I. Bigi, A.I. Sanda, CP Violation, 2nd edn., Cambridge University Press, Cambridge (2009)
12. N. Cabibbo, Unitary symmetry and leptonic decays. Phys. Rev. Lett. **10**, 531–533 (1963)
13. See review on "V_{ud}, V_{us}, the Cabibbo angle and CKM unitarity" in Ref. [49]
14. L.-L. Chau, W.-Y. Keung, Comments on the parametrization of the Kobayashi-Maskawa matrix. Phys. Rev. Lett. **53**, 1802–1805 (1984)
15. L. Wolfenstein, Parametrization of the Kobayashi-Maskawa matrix. Phys. Rev. Lett. **51**, 1945 (1983)
16. C. Jarlskog, Commutator of the quark mass matrices in the standard electroweak model and a measure of maximal CP nonconservation. Phys. Rev. Lett. **55**, 1039–1042 (1985)
17. See review on "The CKM quark-mixing matrix" in Ref. [49]
18. J. Charles et al. (CKMfitter Group), CP violation and the CKM matrix: Assessing the impact of the asymmetric B-factories. Eur. Phys. J. C **41**, 1–131 (2005)
19. M. Bona, M. Ciuchini, E. Franco et al. (UTfit Collaboration), The 2004 UTfit Collaboration report on the status of the Unitarity Triangle in the Standard Model. J. High Energy Phys. **2005**, 028 (2005)
20. V. Weisskopf, E. Wigner, Berechnung der natürlichen Linienbreite auf Grund der Diracschen Lichttheorie. Zeitschrift für Physik **63**, 54–73 (1930)
21. V. Weisskopf, E. Wigner, Über die natürliche Linienbreite in der Strahlung des harmonischen Oszillators. Zeitschrift für Physik **65**, 18–29 (1930)
22. U. Nierste, Three lectures on meson mixing and CKM phenomenology, in Lectures at the Helmholtz International Summer School on Heavy Quark Physics at Dubna (Russia) (2008)
23. J.L. Rosner, B.D. Winstein, Kaon Physics, 1st edn., University of Chicago Press, Chicago (2001)
24. See review on "D^0-$\bar{D}^0$ mixing" in Ref. [49]
25. See review on "B^0-$\bar{B}^0$ mixing" in Ref. [49]
26. A.J. Buras, W. Stominski, H. Steger, B^0-$\bar{B}^0$ mixing, CP violation and the B meson decay. Nucl. Phys. B **245**, 369 (1984)
27. R. Fleischer, Flavour physics and CP violation, Lectures Given at the 2003 European School of High-Energy Physics (2003)
28. A. Einstein, B. Podolsky, N. Rosen, Can quantum-mechanical description of physical reality be considered complete? Phys. Rev. **47**, 777–780 (1935)
29. P. Harrison, H. Quinn, The BaBar Physics Book: Physics at an Asymmetric B-Factory. SLAC-R-504, Stanford Linear Accelerator Center (1998)

30. I.I. Bigi, A.I. Sanda, CP violation in heavy flavor decays: Predictions and search strategies. Nucl. Phys. B **281**, 41–71 (1987)
31. B. Aubert, D. Boutigny, J.-M. Gaillard et al. (BaBar Collaboration), Observation of CP violation in the B^0 meson system. Phys. Rev. Lett. **87**, 091801 (2001)
32. K. Abe, R. Abe, I. Adachi et al. (Belle Collaboration), Observation of large CP violation in the neutral B meson system. Phys. Rev. Lett. **87**, 091802 (2001)
33. D. Asner, S. Banerjee, R. Bernhard et al. (Heavy Flavor Averaging Group), Averages of b-hadron, c-hadron, and τ-lepton properties. arXiv:1010.1589 (2011)
34. M. Meseck, Measurement of the CP-odd fraction in the decay $B^0 \to D^{*+}D^{*-}$ with the Belle experiment. Diploma thesis, Institute for Experimental Nuclear Physics, Karlsruhe Institute of Technology (2010)
35. B. Kronenbitter, Measurement of polarization and CP violation in $B^0 \to D^{*+}D^{*-}$ decays with the Belle detector. Diploma thesis, Institute for Experimental Nuclear Physics, Karlsruhe Institute of Technology (2011)
36. R. Fleischer, Exploring CP violation and penguin effects through $B_d^0 \to D^+D^-$ and $B_s^0 \to D_s^+D_s^-$. Eur. Phys. J. C **51**, 849–858 (2007)
37. M. Gronau, J.L. Rosner, D. Pirjol, Small amplitude effects in $B^0 \to D^+D^-$ and related decays. Phys. Rev. D **78**, 033011 (2008)
38. Z.-Z. Xing, CP violation in $B_d \to D^+D^-$, $D^{*+}D^-$, D^+D^{*-} and $D^{*+}D^{*-}$ decays. Phys. Rev. D **61**, 014010 (1999)
39. M. Gronau, CP violation in neutral B decays to CP eigenstates. Phys. Rev. Lett. **63**, 1451–1454 (1989)
40. B. Grinstein, Critical reanalysis of CP asymmetries in B^0 decays to CP eigenstates. Phys. Lett. B **229**, 280–284 (1989)
41. M. Ciuchini, E. Franco, G. Martinelli et al. CP violating B decays in the Standard Model and supersymmetry. Phys. Rev. Lett. **79**, 978–981 (1997)
42. Y. Grossman, M.P. Worah, CP asymmetries in B decays with new physics in decay amplitudes. Phys. Lett. B **395**, 241–249 (1997)
43. S. Fratina et al. (Belle Collaboration), Evidence for CP violation in $B^0 \to D^+D^-$ decays. Phys. Rev. Lett. **98**, 221802 (2007)
44. B. Aubert, M. Bona, Y. Karyotakis et al. (BaBar Collaboration), Measurements of time-dependent CP asymmetries in $B \to D^{(*)+}D^{(*)-}$ decays. Phys. Rev. D **79**, 032002 (2009)
45. T. Aushev, Y. Iwasaki et al. (Belle Collaboration), Search for CP violation in the decay $B^0 \to D^{*\pm}D^{\mp}$. Phys. Rev. Lett. **93**, 201802 (2004)
46. K. Vervink, T. Aushev, O. Schneider et al. (Belle Collaboration), Evidence of time-dependent CP violation in the decay $B^0 \to D^{*+}D^{*-}$. Phys. Rev. D **80**, 111104 (2009)
47. R. Aleksan, I. Dunietz, B. Kayser et al. CP violation using non-CP eigenstate decays of neutral B mesons. Nucl. Phys. B **361**, 141–165 (1991)
48. B. Aubert, R. Barate, D. Boutigny et al. (BaBar Collaboration), Measurements of branching fractions and CP-violating asymmetries in $B^0 \to \rho^{\pm} h^{\mp}$ decays. Phys. Rev. Lett. **91**, 201802 (2003)
49. K. Nakamura, K. Hagiwara, K. Hikasa et al. (Particle Data Group), Review of particle physics. J. Phys. G **37**, 075021 (2010)

http://www.springer.com/978-3-319-00725-0

Time-Dependent CP Violation Measurements
Analyses of Neutral B Meson to Double-Charm Decays
at the Japanese Belle Experiment
Röhrken, M.
2014, XVIII, 193 p. 82 illus., 40 illus. in color., Hardcover
ISBN: 978-3-319-00725-0